Origin of nitrogen on Mars: First in situ N isotope analyses of martian meteorites

Cécile Deligny, Evelyn Füri, Etienne Deloule, A.H. Peslier, F. Faure, Y. Marrocchi

Origin of nitrogen on Mars: First *in situ* N isotope analyses of martian meteorites

C. Deligny[a,b*], E. Füri[a], E. Deloule[a], A.H. Peslier[c,d], F. Faure[a], Y. Marrocchi[a]

[a] Université de Lorraine, CNRS, CRPG, F-54000 Nancy, France

[b] Department of Geosciences, Swedish Museum of Natural History, Stockholm, Sweden

[c] Jacobs, NASA-Johnson Space Center, Mail Code X13, Houston, TX 77058, USA

[d] Dept. of Geological Sciences, New Mexico State University, Las Cruces, NM 88011, USA

[*] Corresponding author e-mail address: cecile.deligny@nrm.se

This is a post-peer-review, pre-copyedit version of an article published in *Geochimica et Cosmochimica Acta*. The final authenticated version is available online at: https://doi.org/10.1016/j.gca.2023.01.017

ABSTRACT

Martian meteorites are key for assessing the isotopic characteristics of nitrogen in different martian reservoirs (i.e., mantle, crust, and atmosphere), and, ultimately, for constraining the source(s) of nitrogen trapped during the earliest stages of planetary accretion in the terrestrial planet-forming region. In this study, we analysed, for the first time, the nitrogen content and isotopic composition of glassy melt inclusions of Chassigny and of the mesostasis of five nakhlites (MIL 03346, Nakhla, NWA 6148, NWA 998, and Y 000593) by *in situ* secondary ion mass spectrometry. The nitrogen content of Chassigny melt inclusions, corrected for olivine overgrowth on the inclusion walls, varies from 4 ± 1 to 860 ± 45 ppm N, and the majority of $\delta^{15}N$ values range from –35 ± 41 to +73 ± 36‰. The estimated nitrogen isotopic signature of the primitive melt, prior to degassing of N_2 or NH_3, is 0 ± 32‰. The mesostasis of nakhlites contains 2.7 ± 0.2 to 943 ± 156 ppm N, with $\delta^{15}N$ values from –30 ± 37 to +348 ± 43‰. Whereas degassing of N_2 or NH_3 can explain the lowest nitrogen isotopic ratios measured in the nakhlite mesostasis, the ^{15}N-enriched isotopic composition ($\delta^{15}N$ > 150‰) of four nakhlites (MIL 03346, Nakhla, NWA 6148, and Y 000593) likely results from interaction of the mesostasis melt with the martian atmosphere during ejection. The $\delta^{15}N$ values (+25 ± 42 and +77 ± 19‰) of two melt inclusions in Y 000593 are comparable to those of Chassigny, further confirming that these meteorites likely sample a common volatile reservoir in the martian interior. Overall, the new results indicate that the chassignite-nakhlite reservoir did not inherit nitrogen from the solar nebula but, instead, from chondritic-like materials. These findings further confirm that planetary bodies in the inner solar system accreted (isotopically) chondritic nitrogen during the first few million years of solar system history.

Keywords: Mars; Chassigny; Nakhlites; Nitrogen; SIMS; Volatile accretion

1. Introduction

Knowledge of the origin(s) and chronology of accretion of highly volatile elements such as nitrogen and hydrogen on the terrestrial planets is central to our understanding of planetary formation processes and the development of habitable conditions. Earth and Mars presumably formed sunward of the so-called snow line (i.e., the water ice condensation/evaporation front in the protoplanetary disk), in a region where the preservation and accretion of water ice and other N- and H-bearing ices was inhibited (Morbidelli et al., 2000, 2022; Lodders, 2004; Warren, 2011; Hartmann et al., 2017; O'Brien et al., 2018; Bermingham et al., 2020; Lichtenberg et al., 2021; Izidoro et al., 2022). However, the presence of atmospheres, of oceans on Earth, and of water ice in the present polar caps and possibly liquid water between 3.7 and 4.5 Ga on Mars indicates that both of these planets acquired significant amounts of highly volatile elements (e.g., Carr, 2007; Di Achille and Hynek, 2010; Ehlman and Edwards, 2014; Filiberto and Schwenzer, 2018 and references therein; Udry et al., 2020), either during the main stages of planetary growth and/or by late accretion (e.g., Marty, 2012; Hallis et al., 2015; Alexander et al., 2018; Piani et al., 2020).

Mars is a key object to trace the volatile element source(s) in the inner solar system during the early stages of planetary formation. Since no space mission has yet returned samples from Mars, martian meteorites (the so-called SNCs: Shergottites, Nakhlites, Chassignites, as well as ALH (Allan Hills) 84001, NWA (Northwest Africa) 7034, and 16 paired meteorites; Udry et al., 2020) are unique samples to study the formation, differentiation, and evolution of Mars as well as the origin and abundance of volatiles present in the martian interior (McSween, 1994; Filiberto and Schwenzer, 2018; Peslier et al., 2019; Udry et al., 2020). ^{182}Hf-^{182}W and ^{60}Fe-^{60}Ni data suggest that Mars reached half of its size in ~1.8 Ma only (Dauphas and Pourmand, 2011; Tang and Dauphas 2014), and that differentiation and crystallization of its magma ocean was completed ~20–25 Ma after CAI formation (Nimmo and Kleine 2007; Kruijer et al., 2017b, 2020; Bouvier et al., 2018). Due to its small size and rapid accretion, Mars is considered to be a planetary embryo (Dauphas and Pourmand, 2011) and to represent an analogue of Earth during the earliest stages of planet formation. Furthermore, the $\boldsymbol{\varepsilon}^{50}$Ti and $\boldsymbol{\varepsilon}^{54}$Cr values of martian meteorites indicate that Mars accreted within the so-called non-carbonaceous (NC) reservoir, sunward of Jupiter (Leya et al., 2008; Trinquier et al., 2009; Warren, 2011; Kruijer et al., 2020; Kleine et al., 2020). To explain isotopic anomalies of $\boldsymbol{\Delta}^{17}$O, $\boldsymbol{\varepsilon}^{50}$Ti, $\boldsymbol{\varepsilon}^{54}$Cr, $\boldsymbol{\varepsilon}^{62}$Ni, and $\boldsymbol{\varepsilon}^{92}$Mo in martian meteorites, Mars is assumed to have formed from enstatite and ordinary chondrite-like materials (Tang and Dauphas 2014; Brasser et al., 2018 and references therein), likely with a small (~4%) contribution of carbonaceous-chondrite-like (i.e., CC-type) material from the outer solar system (Burkhardt et al., 2021). Consequently, any volatiles trapped and preserved in the martian mantle may originate from various sources in the early inner and outer protoplanetary disk.

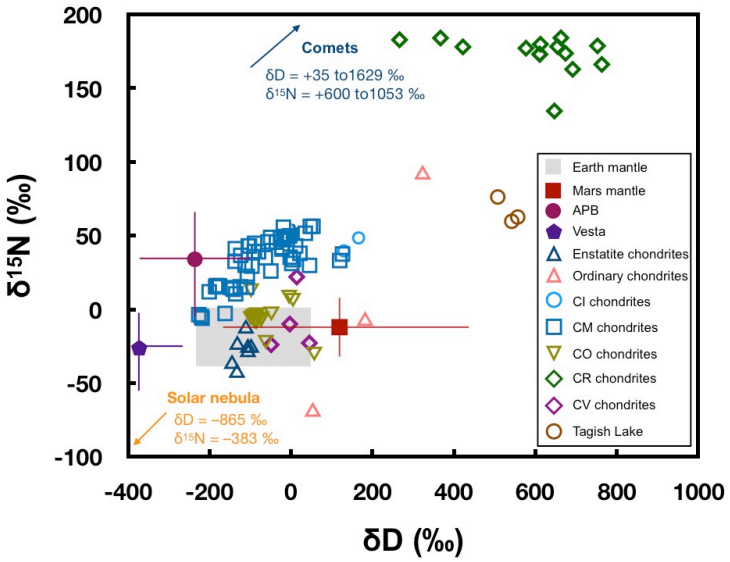

Fig. 1: Nitrogen ($\delta^{15}N$) and hydrogen (δD) isotopic compositions of different objects and reservoirs of the solar system, i.e., Earth's mantle (i.e., *in situ* and whole-rock analyses; Deloule, 1991; Cartigny and Marty, 2013; Hallis et al., 2015; Peslier et al., 2017), Mars' mantle (i.e., *in situ* and whole-rock analyses; Murty et al., 1999; Mathew and Marti, 2001; Gillet et al., 2002; Mohapatra and Murty, 2003; Peslier et al., 2019; Dudley et al., 2022), the angrite parent body (APB) (*in situ* and whole-rock analyses; Abernethy et al., 2013, 2018; Deligny et al., 2021), Vesta (i.e., the parent body of howardites, eucrites, and diogenites (HEDs); *in situ* and whole-rock analyses; Miura and Sugiura, 1993; Abernethy et al., 2018; Stephant et al., 2021), enstatite chondrites (i.e., whole-rock analysis; Kung and Clayton, 1978; Grady et al., 1986; Piani et al., 2020), ordinary chondrites (i.e., whole-rock analysis; McNaughton et al., 1982; Sugiura and Hashizume, 1992; Hashizume et Sugiura, 1995; Alexander et al., 2012; Piani et al., 2021 and references therein), carbonaceous chondrites (i.e., whole-rock analysis; Boato, 1954; Kung and Clayton, 1978; McNaughton et al., 1982; Kerridge, 1985; Grady et al., 1986; Pearson et al., 2001, 2006; Alexander et al., 2012, 2018; Vacher et al., 2020; Piani et al., 2020, 2021 and references therein), and Tagish-Lake (ungrouped carbonaceous chondrites; whole-rock analysis; Alexander et al., 2012) in comparison with the solar nebula (Geiss and Gloeckler, 1998; Marty et al., 2011) as well as Jupiter-family and Oort Cloud comets (i.e., remote measurements of molecules in cometary comae; Arpigny et al., 2003; Biver et al., 2006; Bockelée-Morvan et al., 2012, 2015; Hartogh et al., 2011; Hutsemekers et al., 2008; Jehin et al., 2004, 2009; Manfroid et al., 2005, 2009; Meier et al., 1998; Shinnaka et al., 2016; Villanueva et al., 2008).

Nitrogen and hydrogen isotopes are powerful tools to trace the origin of volatiles accreted by planetary bodies because $^{15}N/^{14}N$ and D/H ratios vary significantly across the solar system. For geochemical applications, nitrogen and hydrogen isotopic ratios are reported as $\delta^{15}N$ and δD values, respectively, where $\delta^{15}N = [(^{15}N/^{14}N_{sample} / {}^{15}N/^{14}N_{atm}) - 1] \times 1{,}000$, in ‰, and the standard is atmospheric N_2 with $^{15}N/^{14}N_{atm} = 3.676 \times 10^{-3}$ (Nier, 1950), and $\delta D = [(D/H_{sample} / D/H_{SMOW}) - 1] \times 1{,}000$), in ‰, and the standard is Standard Mean Ocean Water with $D/H_{SMOW} = 1.557 \times 10^{-4}$ (Gonfiantini, 1978). Space missions, laboratory analyses of meteorites (i.e., bulk and/or *in situ*), and remote observations have permitted to determine the N and H isotopic compositions of various objects in the solar system and to identify three major, isotopically distinct volatile reservoirs (Fig. 1): (i) the solar nebula,

represented by analyses of the solar wind ($\delta^{15}N$ = –383 ± 8‰ and δD = –865‰; Geiss and Gloeckler, 1998; Marty et al., 2011), (ii) chondritic meteorites (e.g., enstatite chondrites (EC) with $\delta^{15}N_{EC}$ = –47 to –13‰ and δD_{EC} = –145 to –98‰; Ivuna-like (CI) and Mighei-like (CM) carbonaceous chondrites with $\delta^{15}N_{CI/CM}$ = –6 to +56‰ and $\delta D_{CI/CM}$ = –227 to +441‰; Boato, 1954; Kung and Clayton, 1978; McNaughton et al., 1982; Kerridge, 1985; Grady et al., 1986; Pearson et al., 2001, 2006; Alexander et al., 2012, 2018; Vacher et al., 2020; Piani et al., 2020, 2021), and (iii) comets ($\delta^{15}N$ = +600 to +1053‰ and δD from +35 to +1629‰; see Deligny et al., 2021 supplementary section). Although cometary $^{15}N/^{14}N$ and D/H ratios have only been determined remotely for a limited number of molecules (i.e., HCN, CN, and NH_2 for $^{15}N/^{14}N$; e.g., Bockelée-Morvan et al., 2015, and references therein), these observations indicate that cometary ices are significantly enriched in the heavy isotopes ^{15}N and D compared to the solar nebula and chondrites. It should also be noted, however, that chondrite groups show a range of nitrogen and hydrogen isotopic compositions because parent body processes (aqueous alteration and/or thermal metamorphism) modified initial isotopic signatures (e.g., Piani et al., 2020; Grewal, 2022).

Previous studies of the water content and hydrogen isotopic composition of SNCs have revealed the presence of three reservoirs with distinct isotopic signatures (e.g., Watson et al., 1994; Leshin, 2000; Boctor et al., 2003; Greenwood et al., 2008; McCubbin et al., 2010, 2016; Hallis et al., 2012; Usui et al., 2012, 2015; Peslier et al., 2019; Barnes et al., 2020; Dudley et al., 2022): i) the mantle: $\delta D \leq -170 \pm 14$ to +430 ± 172‰ (Fig. 1; Gillet et al., 2002; Usui et al., 2012; Peslier et al., 2019; Dudley et al., 2022); ii) the hydrated crust and surficial ice: δD ~1500‰ (Usui et al., 2015); and iii) the atmosphere: δD ~5000‰ (Owen et al., 1988). The range of hydrogen isotopic compositions estimated for the martian mantle is similar to that of CI/CM carbonaceous chondrites, CO- and Tagish Lake-like materials. This implies that primordial water on Mars originates from material accreted in the outer solar system (Desch et al., 2018; Filiberto and Schwenzer, 2018 and references therein). Also, the water contents measured in different groups of martian meteorites are distinct, suggesting that the distribution of water in the martian interior is heterogeneous (Usui et al., 2012; Peslier et al., 2019; Barnes et al., 2020; Dudley et al., 2022).

Nitrogen contents of up to 7450 ppm have been measured by nuclear reaction analysis in melt inclusions of the martian dunite Chassigny (Varela et al., 2000), implying that a large amount of nitrogen could be trapped in Chassigny's mantle source. Mathew and Marti (2001) determined the nitrogen isotopic composition of melt inclusion-bearing olivine separates of Chassigny by step-heating and concluded that a $\delta^{15}N$ value of –30‰ (released at low temperature) may be characteristic of the martian mantle. This value is consistent with the isotopic composition of nitrogen in enstatite chondrites ($\delta^{15}N_{EC}$ = –47 to –13‰; Kung and Clayton, 1978; Grady, 1986). In contrast, nitrogen analysis of fusion-crusted fragments of Nakhla by step heating yielded $\delta^{15}N$ values between +4.6 ± 4.2 and +7.2 ± 3.8‰ (Murty et al., 1999; Mohapatra and Murty, 2003), suggesting that Nakhla is enriched in ^{15}N compared to Chassigny. Finally,

the martian atmosphere, as measured by the Viking lander, was found to contain 2.7 vol.% N_2 with a $\delta^{15}N$ value of +620 ± 160‰ (Owen et al., 1977; Bogard and Johnson, 1983; Owen, 1992; Nyquist et al., 2001). The elevated nitrogen isotopic ratio of the martian atmosphere may either result from ^{14}N loss by non-thermal escape to space (McElroy et al., 1976) or from the contribution of a ^{15}N-rich component such as comets (Marty et al., 2016). All these previous studies highlighted that multiple sources, from the inner and outer solar system, may have contributed nitrogen and hydrogen to Mars.

To better assess the source(s) of volatile elements in the martian interior, we targeted, for the first time, martian meteorites (Chassigny and nakhlites) with well-known ages for nitrogen isotope analyses by *in situ* secondary ion mass spectrometry (SIMS). Melt inclusions, i.e., small pockets of melt encapsulated in minerals during crystal growth, are particularly useful for determining the volatile element composition of primitive, undegassed melts (Sobolev, 1996) and, thus, for assessing the volatile composition of the reservoir that formed the chassignites and nakhlites. The goal of this study was, therefore, to target melt inclusions, but also the mesostasis (glass mixed with silicate minerals or Fe-Ti oxides) that corresponds to the end of the crystallisation sequence, for *in situ* measurements of their nitrogen content and isotopic ratio.

2. Methods

2.1. Sample preparation and imaging

Three sample mounts of Chassigny (2524sp1, 2524sp2, N1142) and two of nakhlites (N1137, P-Mount) were targeted for *in situ* major element and nitrogen analyses in this study (Table S1). Two samples mounted in epoxy (N1142 and N1137) were provided by the Naturhistorisches Museum Wien (NMW). N1142 and N1137 are polished sections of Chassigny and Nakhla, respectively. Two fragments of Chassigny (2 × 10 mg) were provided by the Muséum National d'Histoire Naturelle de Paris (MNHN) and prepared at the Centre de Recherches Pétrographiques et Géochimiques (CRPG, Nancy, France). One chip was polished with ethanol as a lubricant and alumina powder, and pressed into indium (2524sp1). Unfortunately, because Chassigny is highly friable, the majority of melt inclusions (located near fractures) were lost during sample preparation, and only two melt inclusions remained for SIMS analysis. The second fragment was also prepared with ethanol and alumina powder and then mounted in epoxy to prevent the sample from disintegrating (2524sp2). The last sample mount (P-mount) contains separated minerals and mesostasis fragments of five different nakhlites (MIL (Miller Range) 03346, Nakhla, NWA 6148, NWA 998, and Y (Yamato) 000593). This indium mount was prepared without any glue, oil or water, and samples were previously analyzed for major and trace element concentrations, water concentrations, and hydrogen isotope ratios by Peslier et al. (2019). Backscattered and secondary electron

images of all samples were acquired by scanning electron microscopy (SEM; JEOL JSM-6510 at the CRPG) to select areas of interest for subsequent major element and nitrogen analyses.

2.2. Electron Probe Microanalysis (EPMA)

The major and trace element concentrations in pyroxene (i.e., augite and pigeonite), olivine, and mesostasis of the P-mount were reported by Peslier et al. (2019). Major (Si, Al, Fe, Mg, Ca, Na) and minor (Ti, Mn, Cr, K) element compositions of minerals, melt inclusions, and mesostasis in sections N1142 and N1137 were determined during four analytical sessions by EPMA (CAMECA SX-FIVE) at Camparis service (Université Pierre et Marie Curie, Paris, France) using a beam current of 10 nA and an acceleration voltage of 15 kV (Table S2). A suite of natural reference materials was used for calibration and instrument stability monitoring: olivine for Mg and Si, K-feldspars for K and Al, iron oxide for Fe, albite for Na, diopside for Ca, manganese titanite for Mn and Ti, and chromite for Cr. On-peak and background counting times were 40 s for all elements. The quality of all analyses was carefully assessed, and results with totals below 98% or above 102% were discarded. Sections 2524sp1 and 2524sp2 were not analysed by EPMA because the majority of melt inclusions, located near fractures, were lost during sample preparation.

2.3. Secondary Ion Mass Spectrometry (SIMS)

In situ N analyses were performed with the CAMECA 1280-HR2 ion microprobe at CRPG. To minimize terrestrial contamination (i.e., adsorbed water on polished sections), all samples were placed in an oven at 35 °C during ~48 hours before carbon coating (~30 nm thickness). In addition, all polished sections were placed under vacuum in the storage chamber of the SIMS for three days before each analytical session.

A 10 kV Cs^+ primary ion beam with a current of 10 nA was used to measure nitrogen abundances and isotopic ratios following the analytical protocol of Füri et al. (2018). For the analysis of small (≤ 15 µm diameter; Fig. 2C and D) melt inclusions in Chassigny, the primary ion beam intensity was reduced to 2 nA. A normal-incidence electron gun was used for charge compensation. A beam with a raster of 10 × 10 µm was used for 180 s to remove any surface contamination before data acquisition. $^{27}Al^-$ (4 s), $^{30}Si^-$ (4 s), $^{14}N^{16}O^-$ (6 s), $^{15}N^{16}O^-$ (20 s), and $^{16}O_2^-$ (4 s) were measured by peak-jumping in mono-collection mode for twenty-four cycles (~30 min). $^{14}N^{16}O^-$ and $^{15}N^{16}O^-$ signals were measured by ion counting on an electron multiplier, whereas $^{27}Al^-$, $^{30}Si^-$, and $^{16}O_2^-$ were measured on a Faraday cup (FC2). To resolve isobaric interferences induced by the silicon hydrides $^{28}SiH_2^-$ and $^{29}SiH_2^-$ on $^{14}N^{16}O^-$ and $^{15}N^{16}O^-$, respectively, a nominal mass resolution ($m/\Delta m$) of ~12,000 was used. Four analytical sessions were needed for this study. We note that $^{27}Al^-$, which permits to distinguish inclusions from their host mineral,

was not measured in sections N1142 and N1137 during the first SIMS session. However, for all SIMS sessions, the $^{30}Si^-/^{16}O_2^-$ ratio measured in glassy melt inclusions of Chassigny was similar (Table S3). Furthermore, after each analytical session, the location of SIMS spots was assessed by SEM observations. Results from analyses that were not located in the centre of glassy melt inclusions were not considered.

The nitrogen content of minerals, melt inclusions, and mesostasis in all martian meteorites was determined from the $^{14}N^{16}O^-/^{16}O_2^-$ ratio and the known nitrogen content of "dry" basaltic reference glasses synthesized at atmospheric pressure (0.022 ± 0.034 to 3,906 ± 188 ppm N; Fig. S1). This approach has been demonstrated to yield nitrogen abundances (≤1 to 6000 ppm N) in silicate glasses of variable compositions (47.4 to 67.9 wt.% SiO_2) that are in excellent agreement with results from 'bulk' noble gas mass spectrometry analyses (Boulliung et al., 2020). Nitrogen abundances were determined in minerals of Chassigny and nakhlites (n = 5 for each mineral, i.e., olivine, pyroxene), melt inclusions in Chassigny (n = 36), and glassy phases in nakhlites (n = 58, i.e., melt inclusions, mesostasis glass, and mesostasis).

Nitrogen isotopic ratios are only reported for analyses with a significant intensity of $^{14}N^{16}O^-$ ($^{14}N^{16}O^- \geq$ 1,200 cps; $^{15}N^{16}O^- \geq$ 10 cps), equivalent to a nitrogen content ≥ 55 ppm N. The weighted mean $\delta^{15}N$ value of the reference glasses containing ≥ 136 ppm N, as determined from 249 analyses during four analytical sessions, ranges from +19 ± 1.5‰ to +23.2 ± 1.7‰ (Fig. S2). Since their true $\delta^{15}N$ value is –4 ± 1‰ (Füri et al., 2018), all measured isotopic ratios were corrected for an instrumental mass fractionation (Δ_{inst}) of +23‰ to +27.2‰. We note that, at high mass resolution, the presence of silicon hydrides ($^{29}SiH_2^-$) has no effect on the peak intensity of $^{15}N^{16}O^-$ measured in the martian meteorites; i.e., the presence of water does not affect the $\delta^{15}N$ values (Fig. S3B). Phosphates may also affect the measurement of $^{15}N^{16}O^-$ (Deligny et al., 2021); here, the presence of phosphates increases the $^{31}P^-$ peak intensity, but the peak tail does not contribute to the $^{15}N^{16}O^-$ signal (Fig. S3, S4).

2.4. Correction for cosmogenic ^{15}N

Meteoroids are ejected from their parent body as a result of impacts, and, during their transit to Earth, high-energy solar and galactic cosmic rays produce “cosmogenic” (or “spallogenic”) nuclides such as ^{15}N in silicates (Mathew and Murty, 1993). Nitrogen isotopic ratios of the six martian meteorites were corrected for these spallation effects using an average $^{15}N_{cosm}$ production rate of 5.6 $pg \cdot (g\ rock)^{-1} \cdot Ma^{-1}$ (Hashizume et al., 2002). The cosmic ray exposure age of Chassigny is 11.1 ± 1.6 Ma and those of the nakhlites vary from ~10.6 ± 1.0 to 11.3 ± 0.9 Ma (Terribilini et al., 2000; Eugster et al., 2002; Eugster, 2003; Christen et al., 2005; Peslier et al., 2019). Because of the short exposure durations of all martian meteorites, the correction for cosmogenic ^{15}N is small. The maximum correction for measurements with ≤100 ppm N is 19 ‰, i.e. lower than the average 2σ uncertainty on $\delta^{15}N$ of ~33 ‰ (Table S1).

3. Results

3.1. Sample composition and texture

Chassignites (Chassigny, NWA 2737, and NWA 8694) are dunites that crystallized ~1.34 ± 0.05 Ga ago (see Bulletin of the Meteoritical Society; Floran et al., 1978; Varela et al., 2000; Nyquist et al., 2001; Beck et al., 2006; Treiman et al., 2007; Hewins et al., 2020). Chassigny, which supposedly originates from the lower martian crust (Ott, 1988; Swindle, 1995; Mathew and Marti, 2001), consists of highly fractured olivine (~93 vol.%) with minor pyroxene (i.e., pigeonite), feldspar, and troilite. It contains three different types of olivine-hosted melt inclusions of variable sizes: i) completely glassy melt inclusions (Fig. 2C and D); ii) melt inclusions containing a monocrystal of pyroxene (i.e., Ca-poor or Ca-rich pyroxene; Floran et al., 1978; Varela et al., 2000) or chloro-apatite (Fig. 2A and B); and iii) partially crystallized melt inclusions with several mineral phases (Fig. S5; Varela et al., 2000; Varela and Zinner, 2015). The completely glassy, subrounded melt inclusions, ≥ 3 to 30 µm in size, do not contain any bubbles; they were preferentially targeted for SIMS analysis.

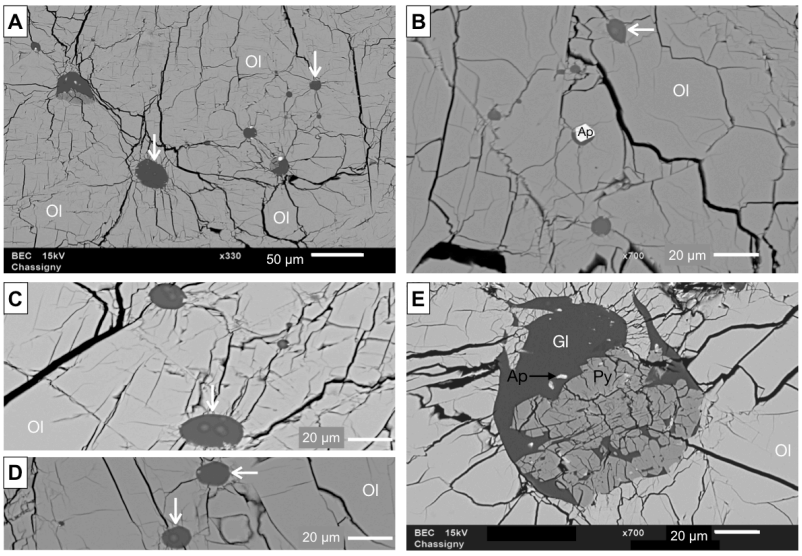

Fig. 2: Backscattered electron images of section N1142 of Chassigny. White arrows indicate completely glassy melt inclusions that were targeted for SIMS analysis (spot size ≤ 10 µm with a 10 × 10 µm raster). (E) Zoom on a peculiar, partially crystallized melt inclusion containing Ca-poor pyroxene and apatite. Partially crystallized melt inclusions were not analyzed. Ap: apatite, Gl: glass, Ol: olivine, Py: pyroxene.

Major element concentrations in glassy melt inclusions in Chassigny (section N1142) are reported in Table S2; they are consistent with those reported by Varela et al. (2000). All analysed glassy melt inclusions have similar major element compositions, and are Si-rich and Mg-poor (65-78 wt.% SiO_2, 17-21 wt.% Al_2O_3, <1.3 wt.% FeO, <0.9 wt.% CaO, <0.7 wt.% MgO; Table S2). The noticeable Mg depletion of the glass can be explained by a post-entrapment modification process (e.g., Sobolev, 1996). Indeed, Floran et al. (1978) argued that the major and minor element compositions of melt inclusions in

Chassigny vary due to the crystallisation (i.e., overgrowth) of olivine on the inclusion walls. The volume fraction (X) of olivine overgrowth in the melt inclusions can be derived from the measured MgO content of olivine ($MgO_{Olivine}$ = 34 ± 0.18 wt.%, on average, Floran et al., 1978) and the glass (i.e., average MgO content measured in melt inclusions; $MgO_{Melt,measured}$ = 0.13 wt.%; Table S2), and the estimated initial MgO content of the primitive melt ($MgO_{Melt,initial}$ ~ 12.6 wt.%; Floran et al., 1978), as follows:

$$MgO_{Melt,initial} = MgO_{Olivine} \times X + MgO_{Melt,measured} \times (1-X)$$

Here, by assuming $MgO_{Melt\ initial}$ = 10 to 15 wt.%, X varies from 0.28 to 0.44, which corresponds to an olivine overgrowth of 0.6 to 2.1 μm in thickness on the walls of the analysed melt inclusions with a radius of 5 to 10 μm. This post-entrapment modification process results in a relative depletion of the residual melt in MgO and an enrichment in SiO_2 and incompatible elements (e.g., N; Section 4.1; Table S2).

Nakhlites (26 meteorites, see Bulletin of the Meteoritical Society) are cumulate rocks that formed ~1.34 ± 0.04 Ga ago (Gale, 1975) in lava flows or shallow intrusions of basaltic magmas (McSween, 2015). They are mainly composed of augite, olivine, and mesostasis (Fig. 3A and B). Nakhla is a peculiar nakhlite because it contains partially crystallized melt inclusions with diameters of up to ~400 μm (Harvey and McSween, 1992; Treiman, 1993). Two melt inclusions of ~150 μm and ~25 μm in size, partially crystallized by clinopyroxene and apatite, were identified in section N1137 of Nakhla (Fig. S6). Completely glassy melt inclusions were not observed in our sections of Nakhla (N1137 and P-mount). The mesostasis of Nakhla consists of glass mixed with apatite, feldspar, and clinopyroxene (Fig. 3B); completely glassy zones, of variable size, were also identified (Fig. 3B). Due to the presence of surrounding minerals, it was not always possible to precisely measure the major element composition of all the glass zones analysed by SIMS. However, one glass patch of ~15 μm diameter (Fig. 3B) in the mesostasis of Nakhla was found to be Si-rich and Mg-poor (75 wt.% SiO_2, 10 wt.% Al_2O_3, 7 wt.% K_2O, 4.3 wt.% FeO, 1.5 wt.% Na_2O, 1 wt.% MgO and CaO), which is consistent with the results of Berkley et al. (1980). The mesostasis of MIL 03346, NWA 6148, and Y 000593 consists of glass (with a plagioclase composition) mixed with Fe-Ti oxides (Fig. 3C and D; Peslier et al., 2019). Melt inclusions were observed in augite and olivine of NWA 6148 and Y 000593 (see Supplementary information in Peslier et al., 2019). Here, melt inclusions, mesostasis glass, and minerals (augite and olivine) of nakhlites were targeted for *in situ* nitrogen analysis by SIMS.

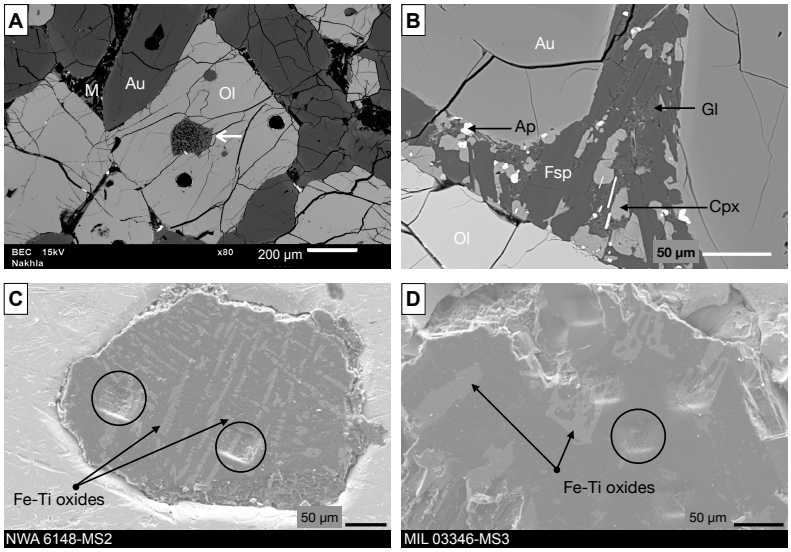

Fig. 3: Backscattered (A, B) and secondary electron images (C, D) of nakhlites. (A) Section N1137 of Nakhla. The white arrow points to a melt inclusion, partially crystallized by clinopyroxene and apatite, that was targeted for SIMS analyses (see section 3.1; spot size ≤ 10 µm with a 10 × 10 µm raster). (B) Mesostasis consisting of glass mixed with apatite, feldspar, and clinopyroxene in Nakhla (section N1137). (C, D) Mesostasis of NWA 6148 and MIL 03346, respectively (P-mount), partially filled with Fe-Ti oxides. Black circles indicate SIMS locations of hydrogen analyses performed by Peslier et al. (2019). Ap: apatite, Au: augite, Fsp: feldspar, Gl: glass, M: mesostasis, Ol: olivine, Cpx: clinopyroxene.

3.2. Nitrogen concentrations and isotopic ratios in Chassigny melt inclusions

Olivine and pyroxene (i.e., pigeonite) in the Chassigny fragment embedded in epoxy contain 20 and 35 ppm N, respectively (sections N1142 and 2524sp2; Table S1). For the sample mounted in indium, the nitrogen contents are ≤ 1 ppm for olivine and ~13 ppm for pyroxene (section 2524sp1; Table S1). This implies that ~20 ppm N in samples mounted in epoxy is derived from degassing of the epoxy and/or contamination during preparation (e.g., polishing). The nitrogen isotopic composition of the contaminant could not be determined; however, assuming an atmospheric $\delta^{15}N$ value of 0 ‰, this contribution would modify $\delta^{15}N$ values by only 3.6‰ for the inclusions with the lowest nitrogen contents (N = 180 and 183 ppm). Therefore, measured nitrogen concentrations and isotopic ratios of olivine-hosted glassy melt inclusions of Chassigny were not corrected for contamination.

The measured nitrogen abundance of olivine-hosted melt inclusions in sections N1142 and 2524sp2 ranges from 6 ± 1 to 1364 ± 71 ppm N (Table S1). Since nitrogen is incompatible in olivine, the nitrogen content of the trapped (residual) melt is expected to have increased as a result of olivine overgrowth along the inclusion walls (section 3.1.). Therefore, we calculated the initial nitrogen content of the melt during its entrapment as inclusions, prior to post-entrapment modification, using the following equation:

$$N_{Melt,initial} = N_{Glass,measured} \times (1\text{-}X),$$

where $N_{Melt,initial}$ and $N_{Glass,measured}$ represent the initial and measured nitrogen contents of the trapped melt, respectively, and X corresponds to the volume fraction of olivine overgrowth (≈ 0.28 to 0.44; see section 3.1). The recalculated 'initial' nitrogen concentrations and associated $\delta^{15}N$ values, are shown in Figure 4. Nitrogen isotopic ratios are not expected to have been affected by this post-entrapment process.

The glassy melt inclusions, which contain ≥180 ppm N (measured abundances), have $\delta^{15}N$ values (corrected for cosmogenic ^{15}N) that vary from –35 ± 41 to +73 ± 36‰ (with the exception of one inclusion that has a higher $\delta^{15}N$ value of +125 ± 43‰). The lowest $\delta^{15}N$ values observed here are remarkably similar to the value of –30‰ obtained by step heating static mass spectrometry analysis of melt inclusion bearing olivine separates from Chassigny (Mathew and Marti, 2001). However, the majority of the melt inclusions analyzed by SIMS are more enriched in ^{15}N compared to the value obtained by Mathew and Marti (2001). Notably, there is no clear correlation between the major element composition (i.e., FeO and MgO) of melt inclusions and their nitrogen contents or isotopic ratios (Fig. S8).

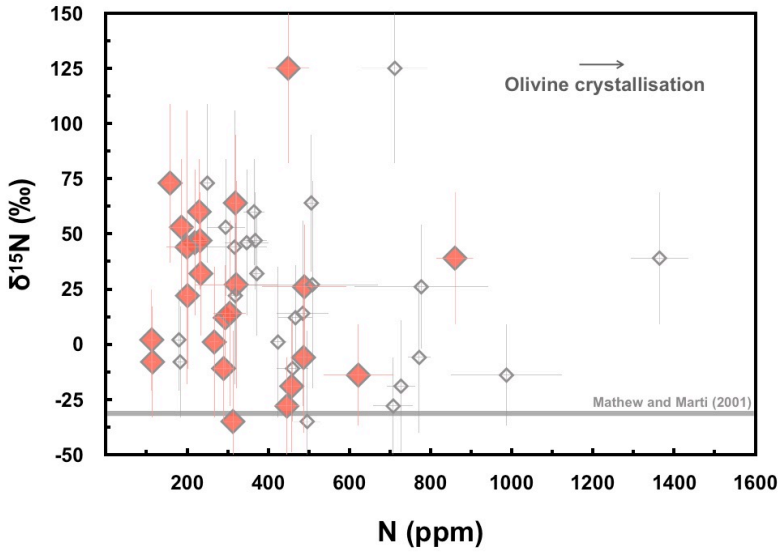

Fig. 4: $\delta^{15}N$ (corrected for cosmogenic ^{15}N; see section 2.4) as a function of the nitrogen concentration (in ppm) in glassy olivine-hosted melt inclusions of Chassigny. Measured nitrogen contents are shown as open grey diamonds, whereas estimated initial nitrogen concentrations, prior to post-entrapment olivine crystallization on the inclusion walls, are shown as filled pink diamonds. Error bars indicate 2σ uncertainties. The $\delta^{15}N$ value of –30‰ obtained previously by step heating analysis of olivine separates of Chassigny (Mathew and Marti, 2001) is indicated by a grey line.

3.3. Nitrogen concentrations and isotopic ratios in melt inclusions and mesostasis of nakhlites

The nitrogen content of olivine and augite in the nakhlites MIL 03346, NWA 6148, and Y 00593 is ≤ 3 ppm N (Table S1). In Nakhla (section N1137 and P-mount), olivine and pyroxene contain ≤ 1.5 ppm N. Despite the different preparation and mounting techniques of the samples (i.e., epoxy *versus* indium), the low nitrogen abundances indicate that there is no detectable nitrogen contamination.

The mesostasis of NWA 998 does not contain enough nitrogen for determining the isotopic composition (≤ 43 ppm N; Table S1; see section 2.3). The nitrogen concentrations in the mesostasis of MIL 03346, Nakhla, NWA 6148, and Y 000593 vary from 2.7 ± 0.2 to 943 ± 156 ppm N, and the $\delta^{15}N$ values range from –30 ± 37 to +348 ± 43‰ (Fig. 5; Table S1). The mesostasis glass in Nakhla was preferentially targeted for SIMS analysis; however, because of the presence of minerals (apatite, feldspar and clinopyroxene; Fig. 3A and B), it was not always possible to target only the glass in the mesostasis. Whereas the 'pure' mesostasis glass of Nakhla contains 52 ± 2 to 421 ± 17 ppm N, the mesostasis (glass and minerals) contains 5 ± 1 to 269 ± 25 ppm N (Table S1). The isotopic composition of nitrogen measured in the mesostasis glass of Nakhla (e.g., –2 ± 35‰) agrees, within error, with the values measured by Murty et al. (1999) in two fusion-crusted fragments of Nakhla by step heating (Fig. 5; $\delta^{15}N$ = +4.6 ± 4.2 to +7.2 ± 3.8‰).

A total of four melt inclusions were found in Nakhla, NWA 6148, and Y 000593. The olivine-hosted inclusion in Nakhla, located near fractures, is partially crystallized by apatite and clinopyroxene (Fig. S6). Its nitrogen content was too low to determine the isotopic composition (≤5 ppm N; n = 3). A second melt inclusion was observed in an augite of NWA 6148 but its nitrogen content was also low (≤ 36 ppm N). Finally, two inclusions were discovered in Y 000593, one in olivine and the other in augite, with nitrogen contents of 531 and 330 ppm N, respectively (Fig. 5; $\delta^{15}N_{\text{Inclusion olivine}}$ = +25 ± 42‰ and $\delta^{15}N_{\text{Inclusion augite}}$ = +77 ± 19‰). The N isotopic composition of these inclusions is similar to that of glassy melt inclusions in Chassigny (Fig. 4).

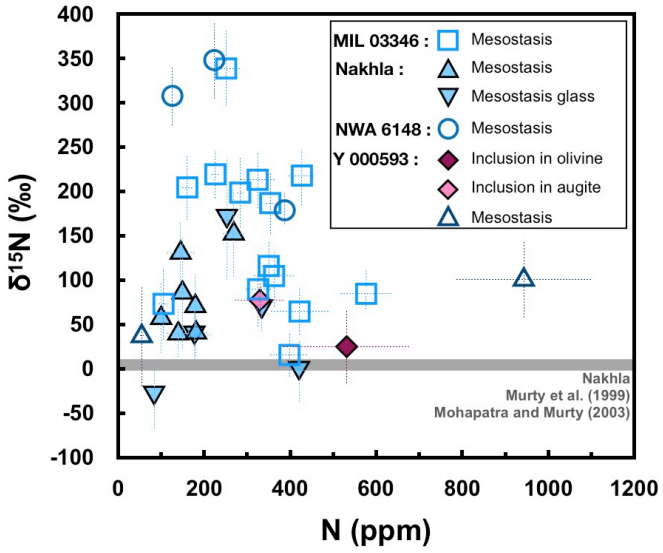

Fig. 5: $\delta^{15}N$ (corrected for cosmogenic ^{15}N; see section 2.4) as a function of the nitrogen content of glasses (i.e., inclusions, mesostasis glass, and mesostasis) in four different nakhlites. Error bars indicate 2σ uncertainties. Previous values for fusion-encrusted Nakhla fragments refer to step heating analyses ($\delta^{15}N$ = +4.6 ± 4.2 to +7.2 ± 3.8‰ corrected for cosmogenic ^{15}N; Murty et al., 1999; Mohapatra and Murty, 2003) and are indicated by a grey bar.

4. Discussion

4.1. Origin and significance of melt inclusions in Chassigny

In this study, only completely glassy melt inclusions trapped in olivine of Chassigny were targeted for nitrogen analyses by SIMS because they are most likely to preserve the volatile composition of the parent melt (see section 3.1). Figure 2 shows that these inclusions are surrounded by numerous radial fractures while the glass itself is unfractured. It is noteworthy that none of the inclusions contain a vapor bubble (this study; Varela et al., 2000), which is in stark contrast to typical mineral-hosted melt inclusions in terrestrial igneous rocks (e.g., Roedder, 1979).

Two previous studies concluded that glassy inclusions in Chassigny are not primary magmatic inclusions that formed and evolved in a closed system (Varela et al., 2000; Varela and Zinner, 2015). Varela et al. (2000) measured the nitrogen content of five glassy and partially crystallized inclusions by nuclear reaction analysis. The nitrogen content was found to vary from 160 to 7450 ppm N with depth within single inclusions, suggesting that nitrogen was heterogeneously distributed in the glass. This nitrogen heterogeneity was interpreted by Varela et al. (2000) to indicate that the inclusions result from heterogeneous trapping of crystals and solid glass precursors from a fluid, and that the host olivine itself is of non-igneous origin. Later, Varela and Zinner (2015) argued that the compositional variability (e.g., N, Na, K, halogens, Rb, Sr) of the glass results from post-formational processes (e.g., metasomatism, metamorphism, shock), suggesting that the inclusions do not preserve a reliable sample of primary melt.

Despite their peculiar characteristics, it has generally been concluded that olivine-hosted glass inclusions in Chassigny have a magmatic origin (e.g., Johnson et al., 1991). In contrast to the findings of Varela et al. (2000), in the samples studied here, nitrogen signals ($^{14}N^{16}O^-$, $^{15}N^{16}O^-$) and also the signals of $^{27}Al^-$, $^{30}Si^-$, and $^{16}O_2^-$ were stable with depth during SIMS analyses of 36 glassy melt inclusions (Fig. S7). Whereas a Cl- and LREE-rich fluid may have been added to the chassignite-nakhlite magma body, melt-inclusion-bearing (cumulus) olivine presumably crystallized prior to this process (McCubbin et al., 2013), implying that the fluid did not modify the nitrogen content and isotopic composition of the trapped melt. Furthermore, although Langenhorst and Greshake (1999) argued that the presence of planar fractures and dislocations in olivine require a shock pressure of 35 GPa, the olivine-hosted glass inclusions are unlikely to be the result of shock metamorphism and melting during the ejection of the meteoroid from Mars because the surrounding fractures do not contain any glass (see Figure 2A, B, C and D; Varela et al., 2000).

The nitrogen, hydrogen, and noble gas (krypton, xenon) isotopic signatures of Chassigny are distinct from the martian atmosphere (this study; Mathew and Marti, 2001; Boctor et al., 2003, Péron and Mukhopadhyay, 2022); melt inclusions are ^{15}N-depleted compared to the isotopic signature of atmospheric nitrogen ($\delta^{15}N$ +620 ± 160‰; Owen et al., 1977; Bogard and Johnson, 1983; Owen, 1992;

Nyquist et al., 2001), demonstrating that nitrogen was not shock-implanted from the atmosphere into trapped melt pockets. Some Chassigny melt inclusions contain a hydrous amphibole that requires a water-rich mantle source (i.e., up to ~250 ppm; Floran et al. 1978; McCubbin et al 2010). Consequently, water must have been stored in the interior of Mars during its primary accretion and differentiation (McCubbin et al., 2010; 2013). Similarly, the chondritic krypton (and xenon) isotopic signature of Chassigny implies that its mantle source contains noble gases that were trapped during the accretion of Mars (Péron and Mukhopadhyay, 2022). Since Mathew and Marti (2001) also concluded that melt inclusions are the carrier phases of the primitive xenon component, glassy melt inclusions permit to better assess the nitrogen composition of the most primitive melt of Chassigny, and, by inference, that of its mantle source.

4.2. Nitrogen isotopic signature of Chassigny's mantle source

The $\delta^{15}N$ values of the majority of glassy melt inclusions in Chassigny vary between –35 ± 41 and +73 ± 36‰ for a wide range of N concentrations (i.e., 113 ± 11 to 860 ± 45 ppm N, recalculated; Fig. 4). However, these values are presumably not directly representative of the nitrogen systematics of Chassigny's parent melt because degassing prior to or during olivine crystallization may have modified the abundance and isotopic composition of dissolved nitrogen. We consider here an open-system degassing model (Rayleigh distillation) to assess if such a process could explain our results (Fig. 6). The solubility and speciation of nitrogen in silicate melt depends on the water content, melt composition, redox conditions (i.e., oxygen fugacity), and pressure (e.g., Libourel et al., 2003; Boulliung et al., 2020; Bernadou et al., 2021). The cumulates sampled by chassignites are assumed to have formed at an oxygen fugacity close to IW (Iron-Wüstite redox buffer) (Lorand et al., 2012 and references therein), suggesting that nitrogen was predominantly dissolved in the form of N_2 (Libourel et al., 2003; Boulliung et al., 2020). However, since Boctor et al. (2003) found water contents of up to 3170 ± 170 ppm in melt inclusions of Chassigny (by SIMS analyses of hydrogen in samples mounted in epoxy), nitrogen could also be dissolved in the form of NH_3 in the melt (Armstrong et al., 2015; Dalou et al., 2019a; Mosenfelder et al., 2019). Because of the lack of information on the physico-chemical conditions prior to olivine crystallization (e.g., pressure, fO_2, fH_2), the speciation of nitrogen in the trapped melt cannot be constrained; therefore, both N_2 and NH_3 species are considered in the degassing model.

Here, we assume that the least-degassed melt is best represented by the glassy melt inclusion with a high nitrogen content of ~622 ppm N (corrected for olivine overgrowth; section 3.2). In this case, the nitrogen isotopic composition of the majority of glassy melt inclusions in Chassigny overlaps, within error, with open system degassing trajectories starting from an initial $\delta^{15}N$ value of 0 ± 32‰. This initial $\delta^{15}N$ value is derived from the probability functions shown in Figure 7, after calculating degassing-

corrected $\delta^{15}N$ values for each melt inclusion (Table S1) using the following equation (Taylor and Sheppard, 1986):

$\delta^{15}N = \delta^{15}N_0 - (1000 + \delta^{15}N_0)(1 - f^{\alpha - 1})$,

where $\delta^{15}N$ and $\delta^{15}N_0$ represent the isotopic compositions of dissolved N after and prior to degassing, respectively, f is the proportion of nitrogen remaining in the melt, and $\boldsymbol{\alpha}$ is the fractionation factor (i.e., $\boldsymbol{\alpha}N_2$ = 1.017 for N_2 loss and $\boldsymbol{\alpha}NH_3$ = 1.028 for NH_3 loss, assuming that isotopic fractionation is proportional to the square root of mass of the isotopologues). Since Chassigny is assumed to contain trapped volatiles that are representative of those incorporated into the interior of Mars during its accretion (e.g., Mathew and Marti, 2001; Boctor et al., 2003; Péron and Mukhopadhyay, 2022), the $\delta^{15}N$ value of 0 ± 32‰ can be used as a source tracer.

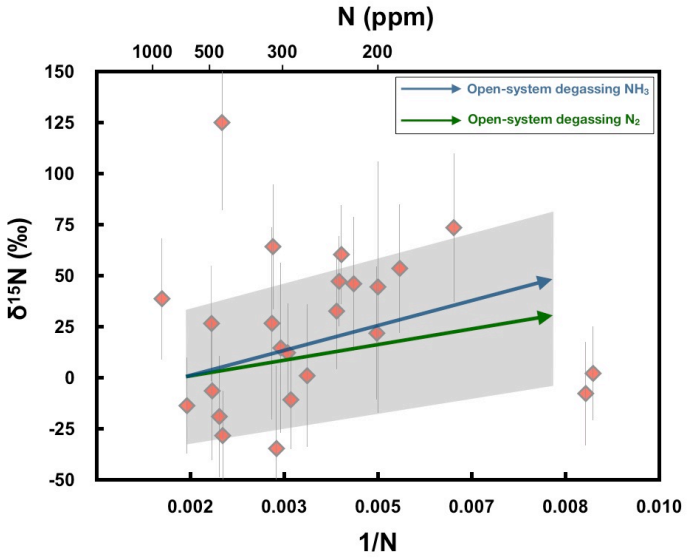

Fig. 6: $\delta^{15}N$ (corrected for cosmogenic ^{15}N; see section 2.4) as a function of the inverse of the nitrogen concentrations (bottom x axis) and the nitrogen concentrations (in ppm; top x axis) in glassy olivine-hosted melt inclusions of Chassigny. Nitrogen concentrations have been corrected for post-entrapment olivine crystallization on the inclusion walls (section 3.2.). Open-system (Rayleigh distillation) degassing trajectories of N_2 (green) and NH_3 (blue) are shown for a melt with an initial N concentration of 622 ppm. Error bars indicate 2σ uncertainties.

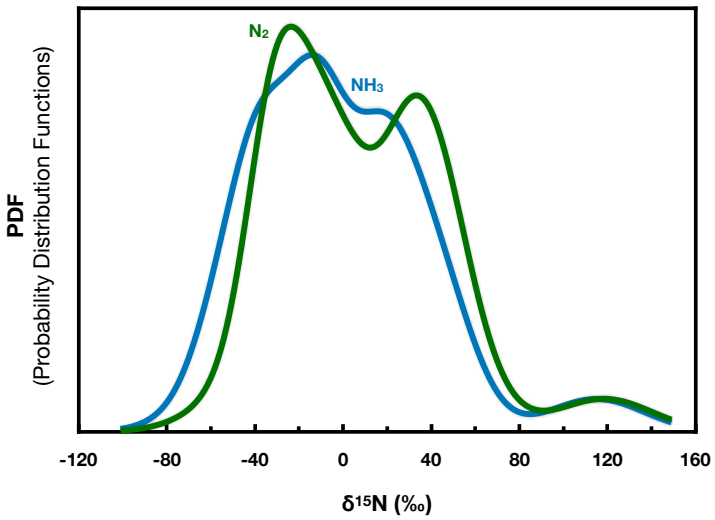

Fig. 7: Calculated initial $\delta^{15}N$ values of the parent melt of Chassigny assuming an initial nitrogen content of 622 ppm. Green and blue curves represent the probability distribution functions of the $\delta^{15}N$ values prior to N_2 and NH_3 degassing (Rayleigh distillation) of the melt, respectively. Chassigny's parent melt is inferred to have had an initial $\delta^{15}N$ value of 0 ± 32‰.

Mathew and Marti (2001) argued that olivine separates of Chassigny have a "solar"-like xenon isotopic signature, which would imply that the martian interior has preserved noble gases that were ingassed during the lifetime of the nebula. However, recent high-precision analyses revealed that krypton (and xenon) isotopic ratios of Chassigny are chondritic (Péron and Mukhopadhyay, 2022). Similarly, our new nitrogen isotope data for olivine-hosted melt inclusions of Chassigny are distinct from solar ($\delta^{15}N$ = –383 ± 8‰; Marty et al., 2011) and comparable to nitrogen in chondritic materials (Fig. 1). In contrast to the inert noble gases, the nitrogen isotopic composition of the martian mantle may have been (slightly) modified by planetary processes (e.g., magma ocean degassing, core formation; Li et al., 2016; Dalou et al. 2019b, 2022). Therefore, the new data do not allow firm conclusions to be drawn on the origin of nitrogen, i.e., nitrogen may originate from enstatite and ordinary chondrite-like materials and/or from carbonaceous chondrite-like material from the outer solar system.

It is noteworthy that similar, but slightly higher, nitrogen isotopic ratios were measured by SIMS in the most primitive melt trapped in the early-formed angrite D'Orbigny (i.e., $\delta^{15}N$ = 0 ± 25 to +56 ± 29‰; Fig. 1; Deligny et al., 2021). Also, eucrites, which are thought to originate from the asteroid Vesta, record $\delta^{15}N$ values between –54.2 ± 14.1 to –2.6 ± 8.8‰ (Fig. 1; Miura and Sugiura, 1993; Abernethy et al., 2018), as revealed by stepped combustion analyses. Finally, nitrogen in the terrestrial mantle has a $\delta^{15}N$ value between –40 and –5‰ (Fig. 1; Cartigny and Marty, 2013); the lowest $\delta^{15}N$ values of –39.4 to –24.9‰ of three diamonds are considered to best represent the isotopic signature of primordial nitrogen in Earth's mantle (Palot et al., 2012). These observations indicate that Earth as well as other early-formed

planetary bodies (i.e., APB, Vesta, and Mars) that accreted sunward Jupiter's orbit incorporated significant quantities of isotopically chondritic nitrogen (e.g., this study; Javoy et al., 1986; Miura and Sugiura, 1993; Abernethy et al., 2018; Deligny et al., 2021).

4.3. Nitrogen isotopic variations in nakhlites

4.3.1. Effect of degassing on the nitrogen isotopic ratios in nakhlites

The similar formation ages, radiogenic isotopic compositions, and ejection ages of the chassignites and nakhlites suggest that these two groups of meteorites originate from the same volcanic area on Mars (Foley et al., 2005; Caro et al., 2008; Debaille et al., 2009; McSween, 2015; Cohen et al., 2017; Udry and Day, 2018; Udry et al., 2020). Also, nakhlites presumably represent a late fractional crystallization product of the chassignite-nakhlite parental magma (Udry and Day, 2018). It is, therefore, important to note that the $\delta^{15}N$ values of the two melt inclusions in Y 000593 ($\delta^{15}N_{\text{Inclusion olivine}}$ = +25 ± 42‰ and $\delta^{15}N_{\text{Inclusion augite}}$ = +77 ± 19‰) are similar to those in Chassigny (Fig. 8). In contrast, the mesostasis in nakhlites has a highly variable nitrogen content and isotopic composition ($\delta^{15}N$ = –30 ± 37 to +348 ± 43‰).

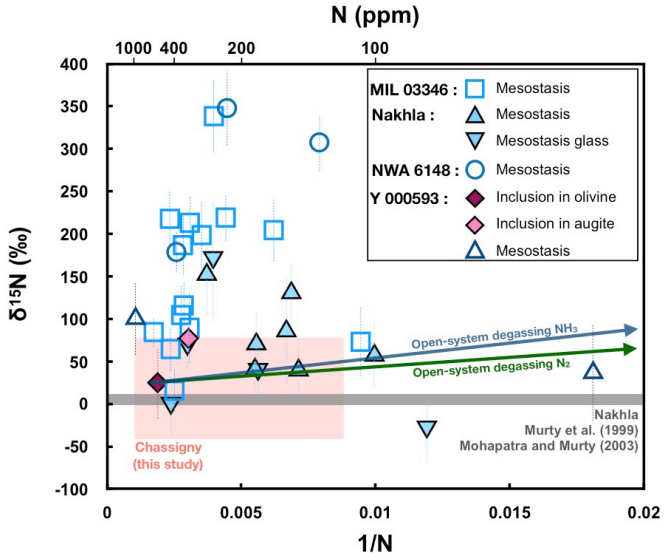

Fig. 8: $\delta^{15}N$ (corrected for cosmogenic ^{15}N; see section 2.4) as a function of the inverse of the nitrogen concentration (bottom x axis) and the nitrogen concentration (in ppm; top x axis) of nakhlites. Trajectories for open-system (Rayleigh distillation) degassing of N_2 and NH_3 are indicated in green and blue, respectively. The range of nitrogen contents (corrected for post-entrapment olivine overgrowth on the inclusion walls) and $\delta^{15}N$ values for Chassigny is indicated by the pink rectangle. Error bars indicate 2σ uncertainties.

To assess if these results can be explained by open-system degassing of the intercumulus melt (i.e., trapped in the form of mesostasis), we applied the same degassing model as for Chassigny (section 4.2.). The nitrogen-rich olivine-hosted melt inclusion of Y 000593 was considered to preserve the most

primitive nitrogen signature of the nakhlite melt. Figure 8 shows that open-system degassing of N_2 or NH_3 can explain the most ^{15}N-depleted values of the mesostasis glass and partially crystallized mesostasis of MIL 03346, Nakhla, and Y 000593, with the exception of one measurement in the mesostasis of Nakhla (N = 84 ± 7 ppm N; $\delta^{15}N$ = –30 ± 37‰). Importantly, however, for all four nakhlites (MIL 03346, Nakhla, NWA 6148, and Y 000593) degassing alone cannot explain the large nitrogen isotopic variations (>150‰). Therefore, other process(es) must have occurred to enrich the mesostatis of these four nakhlites in ^{15}N.

4.3.2. Interaction of the intercumulus melt with hydrothermal fluid(s)

Previous studies showed that the intercumulus melt of nakhlites interacted with an exogenous hydrothermal fluid (Hallis et al., 2012; McCubbin et al., 2013; Shearer et al., 2018). McCubbin et al. (2013) argued that this process occurred during the crystallization of augite, located in intercumulus regions of Chassigny, prior to the formation of the nakhlite reservoir. Similarly, based on the range of chlorine isotopic compositions in Chassigny, Shearer et al. (2018) suggested that a ^{37}Cl-rich fluid infiltrated the chassignite-nakhlite reservoir. Peslier et al. (2019) measured the hydrogen isotopic composition of water in minerals and the mesostasis in nakhlites; they argued that exchange of hydrothermal fluids with the intercumulus melt of nakhlites can explain the range of hydrogen isotopic ratios measured in the mesostasis. Although the origin(s) of the fluid(s) that interacted with the intercumulus melt of nakhlites is still debated (i.e., mantle or crustal origin), the fluid(s) could have modified the speciation and isotopic composition of nitrogen dissolved in the melt.

Theoretical calculations permit to estimate the nitrogen isotope fraction factors for various pairs of molecules at different temperatures (Scalan, 1958; Richet et al., 1977; Hanschmann, 1981; Busigny and Bebout, 2013). For example, the transition from N_2 to NH_3 would induce an isotopic fractionation of +10 to +20‰ at 0°C (Busigny and Bebout, 2013), but the magnitude of isotopic fractionation is expected to be lower at higher temperatures. The small nitrogen isotopic fractionation resulting from the interaction between hydrothermal fluid(s) and the intercumulus melt would, therefore, not be sufficient to explain the highest $\delta^{15}N$ values measured in four nakhlites, with a ^{15}N-enrichment of several hundreds of per mil (Fig. 8).

Alternatively, the fluids could have been in contact with the ^{15}N-rich martian atmosphere ($\delta^{15}N$ = +620 ± 160‰; Owen et al., 1977; Bogard and Johnson, 1983; Owen, 1992; Bogard et al., 2001) prior to their circulation through the chassignite-nakhlite reservoir. However, the hydrogen isotopic composition of the mesostasis of the five nakhlites suggests that the intercumulus melt interacted with a mantle-derived hydrothermal fluid that was isotopically distinct from the surficial reservoirs of Mars (Peslier et al., 2019).

Therefore, interaction of the intercumulus melt in nakhlites with a ^{15}N-rich hydrothermal fluid can likely be ruled out as the cause of the highest $\delta^{15}N$ values measured in the mesostasis of nakhlites.

4.3.3. Interaction of the mesostasis melt with the martian atmosphere

Another process that can account for the ^{15}N-enrichment in the mesostasis of four nakhlites is interaction of the melt with the martian atmosphere during the impact event that ejected the meteoroids from the surface of Mars. Although nakhlites were less affected by shock than Chassigny, the dislocation density in olivine suggests a peak shock pressure of 20 ± 5 GPa (Bunch and Reid, 1975; Greshake, 1998; Nyquist, 2001). Based on an experimental study, Wiens (1988) concluded that a significant amount of noble gases could be trapped in micron-sized vesicles in glassy areas of basalts by shock pressures of 40 GPa. Whereas the implantation efficiency is likely lower at shock pressures between 20 and 35 GPa, experiments revealed that the isotopic composition of shock-implanted gas is similar to the ambient gas phase, implying that mass fractionation is negligible for this mechanism (Bogard et al., 1986).

Glass of shock origin analysed in two basalt-like martian meteorites (shergottites EET790001 and Zagami) has a $\delta^{15}N$ value and $^{40}Ar/^{14}N$ ratio intermediate between those of the primitive signature of Chassigny (this study; Mathew and Marti, 2001) and the martian atmosphere (Bogard et al., 2001). Also, two isotopically distinct xenon components have been detected in Nakhla, one derived from the martian interior and the other from the martian atmosphere (Swindle et al., 1986; Mathew et al., 1998; Murty et al., 1999; Gilmour et al., 2001). Thus, the nitrogen isotopic variations observed in the mesostasis of MIL 03346, Nakhla, NWA 6148, and Y 000593 may be explained by degassing of the intercumulus melt, followed by interaction with the ^{15}N-rich martian atmosphere. It is also noteworthy that an experimental study showed that high pressures favour nitrogen incorporation into silicate melts (Bernadou et al., 2021). Thus, dissolution of atmospheric nitrogen during shock may explain the observation that the highest $\delta^{15}N$ values measured in the mesostasis of nakhlites are associated with nitrogen concentrations between 126 to 427 ppm.

Finally, assimilation of a ^{15}N-rich component during the ejection event may also have increased the nitrogen contents and isotopic ratios in the mesostasis of MIL 03346, Nakhla, NWA 6148, and Y 000593. Various objects formed in the outer solar system have high $\delta^{15}N$ values (Fig. 1). Carbonaceous chondrites such as CR ($\delta^{15}N_{CR}$ = +103 to +184‰; Kerridge, 1985; Pearson et al., 2006; Alexander et al., 2012), CB and CH chondrites ($\delta^{15}N_{CB/CH}$ = +160 to +1000‰; Franchi et al., 1986; Sugiura et al., 2000; Marty et al., 2010), and comets ($\delta^{15}N$ = +600 to +1053‰; see Deligny et al., 2021 supplementary section) have $\delta^{15}N$ values similar to the highest values measured in nakhlites. Hence, it cannot be ruled out that a ^{15}N-rich object from the outer solar system impacted Mars and affected the nitrogen isotopic ratio in the mesostasis of nakhlites upon their ejection.

5. Conclusions

To assess the isotopic signature of nitrogen trapped in the interior of Mars, we determined, for the first time, the nitrogen content and isotopic composition of melt inclusions and mesostatis in martian meteorites (Chassigny and nakhlites) by *in situ* secondary ion mass spectrometry. Analysing small glassy melt inclusions in highly fractured samples such as Chassigny and nakhlites is an analytical challenge. Furthermore, several secondary and planetary processes (i.e., cosmic ray-induced production of ^{15}N, post-entrapment modification, magmatic degassing) likely affected and modified the initial abundance and isotopic composition of nitrogen trapped in martian meteorites. Nonetheless, after corrections for spallation, olivine overgrowth on the melt inclusion walls, and degassing of the melt (N_2 or NH_3), the estimated $\delta^{15}N$ value of the 'primitive' melt trapped in Chassigny is 0 ± 32‰. This value implies that nitrogen trapped in the martian mantle is not inherited from the solar nebula, but, instead, is derived from (isotopically) chondritic material. In contrast, the nitrogen isotopic ratios of the mesostasis of four nakhlites (MIL 03346, Nakhla, NWA 6148, and Y 000593) vary from –30 ± 37 to +348 ± 43‰. Degassing of N_2 or NH_3 alone cannot explain the full range of measured values. Instead, interaction of the mesostasis melt with the martian atmosphere during ejection may explain the nitrogen isotopic variations in nakhlites. Overall, our findings show that the nitrogen isotopic composition of nakhlites was more severely affected by secondary processes than that of Chassigny, although nakhlites are the least shocked of all martian meteorites. Since the exact provenance of Chassigny and nakhlites on Mars remains unknown, a Mars sample-return mission is crucial to collect specific, pristine samples from selected areas of interest on Mars, and, ultimately, to improve our understanding of the origin of volatiles trapped in the interior of Mars.

Declaration of Competing Interest

The authors declare that they have no known competing financial interests or personal relationships that could have appeared to influence the work reported in this paper.

Acknowledgments

We thank Ludovic Ferrière (Naturhistorisches Museum Wien), Emmanuel Jacquet, Matthieu Gounelle, and Mathieu Roskosz (Muséum National D'Histoire Naturelle de Paris) for providing samples of Chassigny and Nakhla. We also thank Richard Hervig, Shuying Yang, Munir Humayun, Jessica Barnes, Anthony Irving, and Alan Brandon for granting the loan of nakhlite samples. Nordine Bouden, Johan Villeneuve, Laurette Piani, Michel Fialin, and Nicolas Rividi are thanked for their assistance during SIMS and EPMA analyses. Lydie Bonal, Ghylaine Quitté, Laurent Remusat, and Maxime Piralla are also thanked for fruitful discussions. We thank Pierre Beck for editorial handling as well as Tomohiro Usui and

two anonymous reviewers for their constructive comments. This work was supported by the European Research Council (ERC) under the European Union's Horizon 2020 research and innovation program (grand agreement no. 715028 to E.F.). AHP was funded by NASA ISFM. This is CRPG contribution XX.

Appendix A. Supplementary Material

Supplementary material includes eight figures (i.e., calibration line of reference materials, isotopic ratios of reference glasses, high-resolution mass spectra at mass 31, BSE maps of the distribution of phosphorus in nakhlites, additional backscattered electron images of Chassigny and Nakha, O_2, Si, Al, ^{14}NO and ^{15}NO signals during SIMS analysis, relationship between FeO, MgO, N content and $\delta^{15}N$ values in Chassigny) and three tables (i.e., research data in a separate excel file, major element composition of glassy melt inclusions in Chasssigny and Al, Si, ^{14}NO, ^{15}NO, and O_2 ,chamber pressure, primary ion beam intensity, Si/O_2 ratio, and the secondary ion intensity ratio $^{14}NO/O_2$ for SIMS analysis).

References

Abernethy F. A. J., Verchovsky A. B., Starkey N. A., Anand M., Franchi I. A. and Grady M. M., 2013. Stable isotope analysis of carbon and nitrogen in angrites. Meteorit. Planet. Sci. 48, 1590–1606.

Abernethy, F.A.J., Verchovsky, A.B., Franchi, I.A. and Grady, M.M., 2018. Basaltic volcanism on the angrite parent body: Comparison with 4 Vesta. *Meteorit. Planet. Sci.* 53, 375-393.

Alexander, C.O.D., Bowden, R., Fogel, M.L., Howard, K.T., Herd, C.D.K., Nittler, L.R., 2012. The provenances of asteroids, and their contributions to the volatile inventories of the terrestrial planets. *Science* 337, 721–723.

Alexander, C.M.D., McKeegan, K.D. and Altwegg, K., 2018. Water reservoirs in small planetary bodies: meteorites, asteroids, and comets. *Space Sci. Rev.* 214, 1-47.

Armstrong, L.S., Hirschmann, M.M., Stanley, B.D., Falksen, E.G., Jacobsen, S.D., 2015. Speciation and solubility of reduced C–O–H–N volatiles in mafic melt: Implications for volcanism, atmospheric evolution, and deep volatile cycles in the terrestrial planets. *Geochim. Cosmochim. Ac*ta 171, 283-302.

Arpigny, C., Jehin, E., Manfroid, J., Hutsemékers, D., Schulz, R., Stüwe, J.A., Zucconi, J.M. and Ilyin, I., 2003. Anomalous nitrogen isotope ratio in comets. *Science* 301, 1522-1524.

Barnes, J.J., McCubbin, F.M., Santos, A.R., Day, J.M., Boyce, J.W., Schwenzer, S.P., Ott, U., Franchi, I.A., Messenger, S., Anand, M. and Agee, C.B., 2020. Multiple early-formed water reservoirs in the interior of Mars. *Nat. Geosci.* 13, 260-264.

Beck, P., Barrat, J.A., Gillet, P., Wadhwa, M., Franchi, I.A., Greenwood, R.C., Bohn, M., Cotten, J., van de Moortèle, B. and Reynard, B., 2006. Petrography and geochemistry of the chassignite Northwest Africa 2737 (NWA 2737). *Geochim. Cosmochim. Acta* 70, 2127-2139.

Berkley, J.L., Keil, K. and Prinz, M., 1980. Comparative petrology and origin of Governador Valadares and other nakhlites. In *Lunar and Planetary Science Conference Proceedings* (Vol. 11, 1089-1102).

Bermingham K.L., Füri, E., Lodders K., Marty, B., 2020. The NC-CC isotope dichotomy: Implications for the chemical and isotopic evolution of the early solar system. *Space Sci. Rev.* 216, 1-29.

Bernadou, F., Gaillard, F., Füri, E., Marrocchi, Y. and Slodczyk, A., 2021. Nitrogen solubility in basaltic silicate melt-Implications for degassing processes. *Chem. Geol.* 573, 120-192.

Biver, N., Bockelée-Morvan, D., Crovisier, J., Lis, D.C., Moreno, R., Colom, P., Henry, F., Herpin, F., Paubert, G. and Womack, M., 2006. Radio wavelength molecular observations of comets C/1999 T1 (McNaught-Hartley), C/2001 A2 (LINEAR), C/2000 WM1 (LINEAR) and 153P/Ikeya-Zhang. *Astron. Astrophys.* 449, 1255-1270.

Boato, G., 1954. The isotopic composition of hydrogen and carbon in the carbonaceous chondrites. *Geochim. Cosmochim. Acta* 6, 209-220.

Bockelée-Morvan, D., Biver, N., Swinyard, B., de Val-Borro, M., Crovisier, J., Hartogh, P., Lis, D.C., Moreno, R., Szutowicz, S., Lellouch, E. and Emprechtinger, M., 2012. Herschel measurements of the D/H and 16O/18O ratios in water in the Oort-cloud comet C/2009 P1 (Garradd). *Astron. Astr.* 544, 15.

Bockelée-Morvan, D., Calmonte, U., Charnley, S., Duprat, J., Engrand, C., Gicquel, A., Hässig, M., Jehin, E., Kawakita, H., Marty, B., Milam, S., 2015. Cometary isotopic measurements. *Space Sci. Rev.* 197, 47-83.

Boctor, N.Z., Alexander, C.O.D., Wang, J. and Hauri, E., 2003. The sources of water in Martian meteorites: Clues from hydrogen isotopes. *Geochim. Cosmochim. Ac*ta 67, 3971-3989.

Bogard, D.D. and Johnson, P., 1983. Martian gases in an Antarctic meteorite? *Science* 221, 651-654.

Bogard, D.D., Hörz, F. and Johnson, P.H., 1986. Shock-implanted noble gases: An experimental study with implications for the origin of Martian gases in shergottite meteorites. *Journal of Geophysical Research: Solid Earth* 91, 99-114.

Bogard, D.D., Clayton, R.N., Marti, K., Owen, T. and Turner, G., 2001. Martian volatiles: isotopic composition, origin, and evolution. *Chronology and evolution of Mars*, 425-458.

Boulliung, J., Füri, E., Dalou, C., Tissandier, L., Zimmermann, L. and Marrocchi, Y., 2020. Oxygen fugacity and melt composition controls on nitrogen solubility in silicate melts. *Geochim. Cosmochim. Ac*ta 284, 120-133.

Bouvier, L.C., Costa, M.M., Connelly, J.N., Jensen, N.K., Wielandt, D., Storey, M., Nemchin, A.A., Whitehouse, M.J., Snape, J.F., Bellucci, J.J. and Moynier, F., 2018. Evidence for extremely rapid magma ocean crystallization and crust formation on Mars. *Nature* 558, 586-589.

Brasser, R., Dauphas, N. and Mojzsis, S.J., 2018. Jupiter's influence on the building blocks of Mars and earth. *Geophys. Res. Lett.* 45, 5908-5917.

Bunch, T.E. and Reid, A.M., 1975. The nakhlites Part I: Petrography and mineral chemistry. *Meteoritics* 10, 303-315.

Burkhardt, C., Spitzer, F., Morbidelli, A., Budde, G., Render, J.H., Kruijer, T.S. and Kleine, T., 2021. Terrestrial planet formation from lost inner solar system material. *Science Adv.* 7, 7601.

Busigny, V. and Bebout, G.E., 2013. Nitrogen in the silicate Earth: Speciation and isotopic behavior during mineral–fluid interactions. *Elements* 9, 353-358.

Carr, M.H., 2007. *The surface of Mars* (Vol. 6). Cambridge University Press.

Caro, G., Bourdon, B., Halliday, A.N. and Quitté, G., 2008. Super-chondritic Sm/Nd ratios in Mars, the Earth and the Moon. *Nature* 452, 336-339.

Cartigny, P., Marty, B., 2013. Nitrogen isotopes and mantle geodynamics: The emergence of life and the atmosphere–crust–mantle connection. *Elements* 9, 359–366.

Christen, F., Eugster, O. and Busemann, H., 2005. Mars ejection times and neutron capture effects of the nakhlites Y000593 and Y000749, the olivine-phyric shergottite Y980459, and the lherzolite NWA1950. Antarct. Meteorite Res. 18, 117-132.

Cohen, B.E., Mark, D.F., Cassata, W.S., Lee, M.R., Tomkinson, T. and Smith, C.L., 2017. Taking the pulse of Mars via dating of a plume-fed volcano. *Nat. Com.* 8, 1-9.

Dalou C., Hirschmann M. M., Jacobsen S. D. and Le Losq C., 2019a. Raman spectroscopy study of COHN speciation in reduced basaltic glasses: implications for reduced planetary mantles. Geochim. Cosmochim. Acta 265, 32–47.

Dalou, C., Füri, E., Deligny, C., Piani, L., Caumon, M.C., Laumonier, M., Boulliung, J., Edén, M., 2019b. Redox control on nitrogen isotope fractionation during planetary core formation. *Proc. Natl. Acad. Sci.* 116, 14485-14494.

Dalou, C., Deligny, C., Füri, E., 2022. Nitrogen isotope fractionation during magma ocean degassing: tracing the composition of early Earth's atmosphere. Geochem. Perspect. Lett. 20, 27–31.

Dauphas, N. and Pourmand, A., 2011. Hf–W–Th evidence for rapid growth of Mars and its status as a planetary embryo. Nature 473, 489.

Debaille, V., Brandon, A.D., Yin, Q.Z. and Jacobsen, B., 2007. Coupled 142 Nd–143 Nd evidence for a protracted magma ocean in Mars. *Nature* 450, 525-528.

Deligny, C., Füri, E. and Deloule, E., 2021. Origin and timing of volatile delivery (N, H) to the angrite parent body: Constraints from in situ analyses of melt inclusions. *Geochim. Cosmochim. Ac*ta 313, 243-256.

Deloule, E., Albarede, F., Sheppard, S.M., 1991. Hydrogen isotope heterogeneities in the mantle from ion probe analysis of amphiboles from ultramafic rocks. *Earth and Planet. Sc. Lett.* 105, 543–553.

Desch, S.J., Kalyaan, A. and Alexander, C.M.D., 2018. The effect of Jupiter's formation on the distribution of refractory elements and inclusions in meteorites. *Astrophysical Journal Supplement Series*, 238, 11.

Di Achille, G. and Hynek, B.M., 2010. Ancient ocean on Mars supported by global distribution of deltas and valleys. *Nat. Geosci.* 3, 459-463.

Dudley, J.M., Peslier, A.H. and Hervig, R.L., 2022. Shock-induced H loss from pyroxene and maskelynite in a Martian meteorite and the mantle source δD of enriched shergottites. *Geochim. Cosmochim. Ac*ta 317, 201-217.

Ehlmann, B.L. and Edwards, C.S., 2014. Mineralogy of the Martian surface. *Annual Review of Earth and Planet. Sc. Lett.* 42, 291-315.

Eugster, O., Busemann, H., Lorenzetti, S. and Terribilini, D., 2002. Ejection ages from krypton- 81-krypton-83 dating and pre-atmospheric sizes of martian meteorites. Meteor. Planet. Sci. 37, 1345-1360.

Eugster, O., 2003. Cosmic-ray exposure ages of meteorites and lunar rocks and their significance. *Geochemistry* 63, 3-30.

Filiberto, J. and Schwenzer, S.P., eds. 2018. *Volatiles in the Martian crust*. Elsevier.

Floran, R.J., Prinz, M., Hlava, P.F., Keil, K., Nehru, C.E. and Hinthorne, J.R., 1978. The Chassigny meteorite: A cumulate dunite with hydrous amphibole-bearing melt inclusions. *Geochim. Cosmochim. Acta* 42, 1213-1229.

Foley, C.N., Wadhwa, M., Borg, L.E., Janney, P.E., Hines, R. and Grove, T.L., 2005. The early differentiation history of Mars from 182W-142Nd isotope systematics in the SNC meteorites. *Geochim. Cosmochim. Acta* 69, 4557-4571.

Franchi, I.A., Wright, I.P., Pillinger, C.T., 1986. Heavy nitrogen in Bencubbin—a light-element isotopic anomaly in a stony-iron meteorite. *Nature* 323, 138-140.

Füri, E., Deloule, E. and Dalou, C., 2018. Nitrogen abundance and isotope analysis of silicate glasses by secondary ionization mass spectrometry. *Chem. Geol.* 493, 327-337.

Gale, N.H., Arden, J.W. and Hutchison, R., 1975. The chronology of the Nakhla achondritic meteorite. *Earth Planet. Sc. Lett.* 26, 195-206.

Geiss, J. and Gloeckler, G., 1998. Abundances of deuterium and helium-3 in the protosolar cloud. *Primordial Nuclei and their Galactic evolution* 239-250.

Gillet, P., Barrat, J.A., Deloule, E., Wadhwa, M., Jambon, A., Sautter, V., Devouard, B., Neuville, D., Benzerara, K. and Lesourd, M., 2002. Aqueous alteration in the Northwest Africa 817 (NWA 817) Martian meteorite. *Earth Planet. Sc. Lett.* 203, 431-444.

Gilmour, J.D., Whitby, J.A. and Turner, G., 2001. Disentangling xenon components in Nakhla: martian atmosphere, spallation and martian interior. Geochim. Cosmochim. Acta 65, 343- 354.

Gonfiantini, R., 1978. Standards for stable isotope measurements in natural compounds. Nature 271, 534-536.

Grady, M.M., Wright, I.P., Carr, L.P., Pillinger, C.T., 1986. Compositional differences in enstatite chondrites based on carbon and nitrogen stable isotope measurements. *Geochim. Cosmochim. Acta* 50, 2799-2813.

Greenwood, J.P., Itoh, S., Sakamoto, N., Vicenzi, E.P. and Yurimoto, H., 2008. Hydrogen isotope evidence for loss of water from Mars through time. *Geophys. Res. Lett.* 35.

Greshake, A., 1998. Transmission electron microscopy characterization of shock defects in minerals from the Nakhla SNC meteorite. *Meteorit. Planet. Sci. Sup.* 33, A63.

Grewal, D.S., 2022. Origin of Nitrogen Isotopic Variations in the Rocky Bodies of the Solar System. *Astrophys. Journal* 937, 123.

Hallis, L.J., Taylor, G.J., Nagashima, K. and Huss, G.R., 2012. Magmatic water in the martian meteorite Nakhla. *Earth and Planet. Sc. Lett.* 359, 84-92.

Hallis, L.J., Huss, G.R., Nagashima, K., Taylor, G.J., Halldórsson, S.A., Hilton, D.R., Mottl, M.J., Meech, K.J., 2015. Evidence for primordial water in Earth's deep mantle. *Science* 350, 795–797.

Hanschmann, G., 1981. Berechnung von isotopieeffekten auf quantenchemischer grundlage am beispiel stickstof fhaltiger molecule. *Zfl-Mitteilungen* 41, 19-39.

Hartmann, L., Ciesla, F., Gressel, O. and Alexander, R., 2017. Disk evolution and the Fate of Water. *Space Sci. Rev.* 212, 813-834.

Hartogh, P., Lis, D.C., Bockelée-Morvan, D., de Val-Borro, M., Biver, N., Küppers, M., Emprechtinger, M., Bergin, E.A., Crovisier, J., Rengel, M. and Moreno, R., 2011. Ocean-like water in the Jupiter-family comet 103P/Hartley 2. *Nature* 478, 218-220.

Harvey, R.P. and McSween Jr, H.Y., 1992. Petrogenesis of the nakhlite meteorites: Evidence from cumulate mineral zoning. *Geochim. Cosmochim. Ac*ta 56, 1655-1663.

Hashizume, K. and Sugiura, N., 1995. Nitrogen isotopes in bulk ordinary chondrites. *Geochim. Cosmochim. Ac*ta 59, 4057-4069.

Hashizume, K., Marty, B., Wieler, R., 2002. Analyses of nitrogen and argon in single lunar grains: towards a quantification of the asteroidal contribution to planetary surfaces. *Earth and Planet. Sc. Lett.* 202, 201–216.

Hewins, R.H., Humayun, M., Barrat, J.A., Zanda, B., Lorand, J.P., Pont, S., Assayag, N., Cartigny, P., Yang, S. and Sautter, V., 2020. Northwest Africa 8694, a ferroan chassignite: Bridging the gap between nakhlites and chassignites. *Geochim. Cosmochim. Ac*ta 282, 201-226.

Hutsemekers, D., Manfroid, J., Jehin, E., Zucconi, J.M. and Arpigny, C., 2008. The OH/OH and OD/OH isotope ratios in comet C/2002 T7 (LINEAR). *Astron. Astrophys.* 490, L31-L34.

Izidoro, A., Dasgupta, R., Raymond, S.N., Deienno, R., Bitsch, B. and Isella, A., 2022. Planetesimal rings as the cause of the Solar System's planetary architecture. *Nature Astronomy*, 6, 357-366.

Javoy, M., Pineau, F., Delorme, H., 1986. Carbon and nitrogen isotopes in the mantle. Chem. Geol. 57, 41–62.

Jehin, E., Manfroid, J., Cochran, A.L., Arpigny, C., Zucconi, J.M., Hutsemekers, D., Cochran, W.D., Endl, M. and Schulz, R., 2004. The anomalous 14N/15N ratio in comets 122P/1995 S1 (de Vico) and 153P/2002 C1 (Ikeya-Zhang). *Astrophys. J. Lett.* 613, L161.

Jehin, E., Manfroid, J., Hutsemekers, D., Arpigny, C. and Zucconi, J.M., 2009. Isotopic ratios in comets: status and perspectives. *Earth Moon Planets* 105, 167-180.

Johnson, M.C., Rutherford, M.J. and Hess, P.C., 1991. Chassigny petrogenesis: melt compositions, intensive parameters and water contents of Martian (?) magmas. *Geochim. Cosmochim. Ac*ta 55, 349-366.

Kerridge, J.F., 1985. Carbon, hydrogen and nitrogen in carbonaceous chondrites: Abundances and isotopic compositions in bulk samples. *Geochim. Cosmochim. Acta* 49, 1707-1714.

Kleine, T., Budde, G., Burkhardt, C., Kruijer, T.S., Worsham, E.A., Morbidelli, A., Nimmo, F., 2020. The Non-carbonaceous–Carbonaceous Meteorite Dichotomy. *Space Sci. Rev*. 216, 1-27.

Kruijer, T.S., Kleine, T., Borg, L.E., Brennecka, G.A., Irving, A.J., Bischoff, A. and Agee, C.B., 2017. The early differentiation of Mars inferred from Hf–W chronometry. *Earth and Planet. Sc. Lett.* 474, 345-354.

Kruijer, T.S., Kleine, T., Borg, L.E., 2020. The great isotopic dichotomy of the early Solar System. *Nature Astronomy*, 1-9.

Kung, C.C. and Clayton, R.N., 1978. Nitrogen abundances and isotopic compositions in stony meteorites. *Earth and Planet. Sc. Lett.* 38, 421-435.

Langenhorst, F. and Greshake, A., 1999. A transmission electron microscope study of Chassigny: Evidence for strong shock metamorphism. *Meteorit. Planet. Sci.* 34, 43-48.

Leshin, L.A., 2000. Insights into martian water reservoirs from analyses of martian meteorite QUE94201. *Geophys. Res. Lett.* 27, 2017-2020.

Leya, I., Schönbächler, M., Wiechert, U., Krähenbühl, U. and Halliday, A.N., 2008. Titanium isotopes and the radial heterogeneity of the solar system. *Earth Planet. Sc. Lett.* 266, 233-244.

Li, Y.F., Marty, B., Shcheka, S., Zimmermann, L. and Keppler, H., 2016. Nitrogen isotope fractionation during terrestrial core-mantle separation. *Geochem. Perspect. Lett.* 2, 138-147.

Libourel, G., Marty, B. and Humbert, F., 2003. Nitrogen solubility in basaltic melt. Part I. Effect of oxygen fugacity. *Geochim. Cosmochim. Ac*ta 67, 4123-4135.

Lichtenberg, T., Drążkowska, J., Schönbächler, M., Golabek, G.J. and Hands, T.O., 2021. Bifurcation of planetary building blocks during Solar System formation. *Science* 371, 365-370.

Lodders, K., 2004. Jupiter formed with more tar than ice. *Astrophys. J.* 611, 587.

Lorand, J.P., Pont, S., Chevrier, V., Luguet, A., Zanda, B. and Hewins, R., 2018. Petrogenesis of martian sulfides in the Chassigny meteorite. *Am. Mineral. Journal of Earth and Planetary Materials* 103, 872-885.

Manfroid, J., Jehin, E., Hutsemékers, D., Cochran, A., Zucconi, J.M., Arpigny, C., Schulz, R. and Stüwe, J.A., 2005. Isotopic abundance of nitrogen and carbon in distant comets. *Astron. Astrophys.* 432, L5-L8.

Manfroid, J., Jehin, E., Hutsemékers, D., Cochran, A., Zucconi, J.M., Arpigny, C., Schulz, R., Stüwe, J.A. and Ilyin, I., 2009. The CN isotopic ratios in comets. *Astron. Astrophys*. 503, 613-624.

Marty, B., Kelley, S., Turner, G., 2010. Chronology and shock history of the Bencubbin meteorite: a nitrogen, noble gas, and Ar–Ar investigation of silicates, metal and fluid inclusions. *Geochim. Cosmochim. Acta* 74, 6636-6653.

Marty, B., Chaussidon, M., Wiens, R.C., Jurewicz, A.J.G., Burnett, D.S., 2011. A ^{15}N-poor isotopic composition for the solar system as shown by Genesis solar wind samples. *Science* 332, 1533-1536.

Marty, B., 2012. The origins and concentrations of water, carbon, nitrogen and noble gases on Earth. *Earth and Planet. Sci. Lett.* 313, 56-66.

Marty B., Avice G., Sano Y., Altwegg K., Balsiger H., Hässig M., Morbidelli A., Mousis O. and Rubin M., 2016. Origins of volatile elements (H, C, N, noble gases) on Earth and Mars in light of recent results from the ROSETTA cometary mission. *Earth Planet. Sc. Lett.* 441, 91–102.

Mathew, K.J. and Murty, S.V.S., 1993. Cosmic ray produced nitrogen in extra terrestrial matter. *Proceedings of the Indian Academy of Sciences-Earth and Planetary Sciences* 102, 415-437.

Mathew, K.J., Kim, J.S. and Marti, K., 1998. Martian atmospheric and indigenous components of xenon and nitrogen in the Shergotty, Nakhla, and Chassigny group meteorites. *Meteorit. Planet. Sci.*, 33, 655-664.

Mathew, K.J. and Marti, K., 2001. Early evolution of Martian volatiles: Nitrogen and noble gas components in ALH84001 and Chassigny. *J. Geophys. Res-Planet*. 106, 1401-1422.

McCubbin, F.M., Smirnov, A., Nekvasil, H., Wang, J., Hauri, E. and Lindsley, D.H., 2010. Hydrous magmatism on Mars: A source of water for the surface and subsurface during the Amazonian. *Earth and Planet. Sc. Lett.* 292, 132-138.

McCubbin, F.M., Elardo, S.M., Shearer Jr, C.K., Smirnov, A., Hauri, E.H. and Draper, D.S., 2013. A petrogenetic model for the comagmatic origin of chassignites and nakhlites: Inferences from chlorine-rich minerals, petrology, and geochemistry. *Meteorit. Planet. Sci.* 48, 819-853.

McCubbin, F.M., Boyce, J.W., Srinivasan, P., Santos, A.R., Elardo, S.M., Filiberto, J., Steele, A. and Shearer, C.K., 2016. Heterogeneous distribution of H2O in the Martian interior: Implications for the abundance of H2O in depleted and enriched mantle sources. *Meteorit. Planet. Sci.* 51, 2036-2060.

McElroy, M.B., Yung, Y.L. and Nier, A.O., 1976. Isotopic composition of nitrogen: Implications for the past history of Mars' atmosphere. *Science* 194, 70-72.

McNaughton, N.J., Borthwick, J., Fallick, A.E. and Pillinger, C.T., 1982. Deuterium enrichments in primitive meteorites. In *Lunar and Planetary Science Conference* 13, 501-502.

McSween Jr, H.Y., 1994. What we have learned about Mars from SNC meteorites. *Meteoritics* 29, 757-779.

McSween Jr, H.Y., 2015. Petrology on mars. *Am. Mineral.* 100, 2380-2395.

Meier, R., Owen, T.C., Matthews, H.E., Jewitt, D.C., Bockelée-Morvan, D., Biver, N., Crovisier, J. and Gautier, D., 1998. A determination of the HDO/H2O ratio in comet C/1995 O1 (Hale-Bopp). *Science* 279, 842-844.

Miura, Y. and Sugiura, N., 1993. Nitrogen isotopic compositions in three Antarctic and two non-Antarctic eucrites. *Antarctic Meteorite Research*, 6, 338.

Mohapatra, R.K. and Murty, S.V.S., 2003. Precursors of Mars: Constraints from nitrogen and oxygen isotopic compositions of martian meteorites. *Meteorit. Planet. Sci.* 38, 225-241.

Mosenfelder, J.L., Von Der Handt, A., Füri, E., Dalou, C., Hervig, R.L., Rossman, G.R., Hirschmann, M.M., 2019. Nitrogen incorporation in silicates and metals: Results from SIMS, EPMA, FTIR, and laser-extraction mass spectrometry. *Am. Mineral.* 104, 31-46.

Morbidelli, A., Chambers, J., Lunine, J.I., Petit, J.M., Robert, F., Valsecchi, G.B. and Cyr, K.E., 2000. Source regions and timescales for the delivery of water to the Earth. *Meteoritics & Planetary Science* 35,1309-1320.

Morbidelli, A., Baillie, K., Batygin, K., Charnoz, S., Guillot, T., Rubie, D.C. and Kleine, T., 2022. Contemporary formation of early Solar System planetesimals at two distinct radial locations. *Nature Astronomy* 6, 72-79.

Murty, S.V.S., Mohapatra, R.K., Goswami, J.N. and Sinha, N., 1999. Cosmogenic records and trapped gases in the Nakhla meteorite. *Meteorit. Planet. Sci. Sup.* 34, A84.

Nier, A., 1950. A redetermination of the relative abundances of the isotopes of carbon, nitrogen, oxygen, argon, and potassium. *Phys. Rev.* 77, 789–793.

Nimmo, F. and Kleine, T., 2007. How rapidly did Mars accrete? Uncertainties in the Hf–W timing of core formation. *Icarus* 191, 497-504.

Nyquist, L.E., Bogard, D.D., Shih, C.Y., Greshake, A., Stöffler, D. and Eugster, O., 2001. Ages and geologic histories of Martian meteorites. *Chronology and evolution of Mars* 105-164.

O'Brien, D.P., Izidoro, A., Jacobson, S.A., Raymond, S.N. and Rubie, D.C., 2018. The delivery of water during terrestrial planet formation. *Space Sci. Rev.* 214, 1-24.

Ott, U., 1988. Noble gases in SNC meteorites: Shergotty, Nakhla, Chassigny. *Geochim. Cosmochim. Acta* 52, 1937-1948.

Owen, T., Biemann, K., Rushneck, D.R., Biller, J.E., Howarth, D.W. and Lafleur, A.L., 1977. The composition of the atmosphere at the surface of Mars. *Journal of Geophysical research*, 82, 4635-4639.

Owen, T., Maillard, J.P., De Bergh, C. and Lutz, B.L., 1988. Deuterium on Mars: The abundance of HDO and the value of D/H. *Science* 240, 1767-1767.

Owen, T., 1992. The composition and early history of the atmosphere of Mars. *Mars* 818-834.

Palot M., Cartigny P., Harris J. W., Kaminsky F. V. and Stachel T., 2012. Evidence for deep mantle convection and primordial heterogeneity from nitrogen and carbon stable isotopes in diamond. *Earth Planet. Sc. Lett.* 357–358, 179–193. Pearson, V.K., Sephton, M.A., Gilmour, I., Franchi, I., 2001. Hydrogen isotopic composition of the Tagish Lake meteorite: comparison with other carbonaceous chondrites. *32nd Annual Lunar and Planetary Science Conference*, abstract no. 1861.

Pearson, V.K., Sephton, M.A., Franchi, I.A., Gibson, J.M. and Gilmour, I., 2006. Carbon and nitrogen in carbonaceous chondrites: Elemental abundances and stable isotopic compositions. *Meteorit. Planet. Sci.* 41, 1899-1918.

Péron, S. and Mukhopadhyay, S., 2022. Krypton in the Chassigny meteorite shows Mars accreted chondritic volatiles before nebular gases. *Science* p.eabk1175.

Peslier, A.H., Schönbächler, M., Busemann, H., Karato, S.I., 2017. Water in the Earth's interior: Distribution and origin. *Space Sci. Rev.* 212, 743-810.

Peslier, A.H., Hervig, R., Yang, S., Humayun, M., Barnes, J.J., Irving, A.J. and Brandon, A.D., 2019. Determination of the water content and D/H ratio of the martian mantle by unraveling degassing and crystallization effects in nakhlites. *Geochim. Cosmochim. Acta* 266, 382-415.

Piani, L., Marrocchi, Y., Rigaudier, T., Vacher, L.G., Thomassin, D., Marty, B., 2020. Earth's water may have been inherited from material similar to enstatite chondrite meteorites. *Science* 369, 1110-1113.

Piani, L., Marrocchi, Y., Vacher, L.G., Yurimoto, H. and Bizzarro, M., 2021. Origin of hydrogen isotopic variations in chondritic water and organics. *Earth and Planet. Sc. Lett.* 567, 117008.

Richet P, Bottinga Y, Javoy M., 1977. A review of hydrogen, carbon, nitrogen, oxygen, sulphur and chlorine stable isotope fractionation among gaseous molecules. Annual Review of *Earth Planet. Sc. Lett.* 5: 65-110.

Roedder, E., 1979. Origin and significance of magmatic inclusions. *Bulletin de Mineralogie* 102, 487-510.

Scalan, R.S., 1958. *The isotopic composition, concentration, and chemical state of the nitrogen in igneous rocks* (Doctoral dissertation, University of Arkansas, Fayetteville).

Shearer, C.K., Messenger, S., Sharp, Z.D., Burger, P.V., Nguyen, A.N. and McCubbin, F.M., 2018). Distinct chlorine isotopic reservoirs on Mars. Implications for character, extent and relative timing of crustal interactions with mantle-derived magmas, evolution of the martian atmosphere, and the building blocks of an early Mars. *Geochim. Cosmochim. Acta* 234, 24-36.

Shinnaka, Y., Kawakita, H., Jehin, E., Decock, A., Hutsemékers, D., Manfroid, J. and Arai, A., 2016. Nitrogen isotopic ratios of NH2 in comets: implication for 15N-fractionation in cometary ammonia. *Mon. Not. R. Astron. Soc.* 462, S195-S209.

Sobolev, A.V., 1996. Melt inclusions in minerals as a source of principle petrological information. *Petrology* 4, 209-220.

Stephant, A., Wadhwa, M., Hervig, R., Bose, M., Zhao, X., Barrett, T.J., Anand, M. and Franchi, I.A., 2021. A deuterium-poor water reservoir in the asteroid 4 Vesta and the inner solar system. *Geochim. Cosmochim. Acta* 297, 203-219.

Sugiura, N. and Hashizume, K., 1992. Nitrogen isotope anomalies in primitive ordinary chondrites. *Earth and Planet. Sc. Lett.* 111, 441-454.

Sugiura, N., Zashu, S., Weisberg, M., Prinz, M., 2000. A nitrogen isotope study of bencubbinites. *Meteorit. Planet. Sci*. 35, 987-996.

Swindle, T.D., Burkland, M.K., Grier, J.A., Lindstrom, D.L. and Treiman, A.H., 1995. Noble gas analysis and INAA of aqueous alteration products from the Lafayette meteorite: Liquid water on Mars< 350 Ma ago. In *Lunar and Planetary Science Conference* (Vol. 26).

Swindle, T.D. and Jones, J.H., 1997. The xenon isotopic composition of the primordial Martian atmosphere: Contributions from solar and fission components. *J. Geophys. Res-Planet*. 102, 1671-1678.

Tang, H. and Dauphas, N., 2014. 60Fe–60Ni chronology of core formation in Mars. *Earth and Planet. Sc. Lett.* 390, 264-274.

Taylor, H.P. and Sheppard, S.M.F., 1986. Igneous rocks: I. Processes of isotopic fractionation and isotopic systematics, in: Valley, J.W., Taylor, H.P., O'Neil, J.R. (Eds.), Stable isotopes. Mineralogical Society of America, 227-272.

Terribilini, D., Busemann, H. and Eugster, O., 2000. Krypton-81-Krypton CRE ages of martian meteorites including the new shergottite Los Angeles. Meteor. Planet. Sci. 35.

Treiman, A.H., 1993. The parent magma of the Nakhla (SNC) meteorite, inferred from magmatic inclusions. *Geochim. Cosmochim. Ac*ta 57, 4753-4767.

Treiman, A.H., Dyar, M.D., McCanta, M., Noble, S.K. and Pieters, C.M., 2007. Martian Dunite NWA 2737: Petrographic constraints on geological history, shock events, and olivine color. *J. Geophys. Res: Planets*, *112*(E4).

Trinquier, A., Elliott, T., Ulfbeck, D., Coath, C., Krot, A.N., Bizzarro, M., 2009. Origin of nucleosynthetic isotope heterogeneity in the solar protoplanetary disk. *Science* 324, 374–376.

Udry, A. and Day, J.M., 2018. 1.34 billion-year-old magmatism on Mars evaluated from the co-genetic nakhlite and chassignite meteorites. *Geochim. Cosmochim. Acta* 238, 292-315.

Udry, A., Howarth, G.H., Herd, C.D.K., Day, J.M., Lapen, T.J. and Filiberto, J., 2020. What martian meteorites reveal about the interior and surface of Mars. *J. Geophys. Res-Planet*. 125, 2020JE006523.

Usui, T., Alexander, C.M.D., Wang, J., Simon, J.I. and Jones, J.H., 2012. Origin of water and mantle–crust interactions on Mars inferred from hydrogen isotopes and volatile element abundances of olivine-hosted melt inclusions of primitive shergottites. *Earth and Planet. Sc. Lett.* 357, 119-129.

Usui, T., Alexander, C.M.D., Wang, J., Simon, J.I. and Jones, J.H., 2015. Meteoritic evidence for a previously unrecognized hydrogen reservoir on Mars. *Earth and Planet. Sc. Lett.* 410, 140-151.

Vacher, L.G., Piani, L., Rigaudier, T., Thomassin, D., Florin, G., Piralla, M. and Marrocchi, Y., 2020. Hydrogen in chondrites: Influence of parent body alteration and atmospheric contamination on primordial components. *Geochim. Cosmochim. Ac*ta 281, 53-66.

Varela, M.E., Kurat, G., Bonnin-Mosbah, M., Clocchiatti, R. and Massare, D., 2000. Glass-bearing inclusions in olivine of the Chassigny achondrite: Heterogeneous trapping at sub-igneous temperatures. *Meteorit. Planet. Sci.* 35, 39-52.

Varela, M.E. and Zinner, E., 2015. Glass-bearing inclusions in Shergotty and Chassigny: Consistent samples of a primary trapped melt?. *Meteorit. Planet. Sci.* 50, 2045-2066.

Villanueva, G.L., Mumma, M.J., Bonev, B.P., DiSanti, M.A., Gibb, E.L., Böhnhardt, H. and Lippi, M., 2008. A sensitive search for deuterated water in comet 8P/Tuttle. *Astrophys. J. Lett.* 690, L5.

Warren, P.H., 2011. Stable-isotopic anomalies and the accretionary assemblage of the Earth and Mars: A subordinate role for carbonaceous chondrites. *Earth and Planet. Sc. Lett.* 311, 93–100.

Watson, L.L., Hutcheon, I.D., Epstein, S. and Stolper, E.M., 1994. Water on Mars: Clues from deuterium/hydrogen and water contents of hydrous phases in SNC meteorites. *Science*, 265, 86-90.

Wiens, R.C., 1988. On the siting of gases shock-emplaced from internal cavities in basalt. *Geochim. Cosmochim. Ac*ta 52, 2775-2783.